New Insights on Ecosystem Mercury Cycling Revealed by Stable Isotopes of Mercury in Water Flowing from a Headwater Peatland Catchment

By: Glenn E. Woerndle, Martin Tsz-Ki Tsui, Stephen D. Sebestyen, Joel D. Blum, Xiangping Nie, and Randall K. Kolka

Woerndle, Glenn E.; Tsz-Ki Tsui, Martin; Sebestyen, Stephen D.; Blum, Joel D.; Nie, Xiangping; Kolka, Randall K. New Insights on Ecosystem Mercury Cycling Revealed by Stable Isotopes of Mercury in Water Flowing from a Headwater Peatland Catchment. Environmental Science and Technology. v52 n4 (Feb 20, 2018) 1854-1861.
https://doi.org/10.1021/acs.est.7b04449

Abstract:

Stable isotope compositions of mercury (Hg) were measured in the outlet stream and in soil cores at different landscape positions in a 9.7-ha boreal upland-peatland catchment. An acidic permanganate/persulfate digestion procedure was validated for water samples with high dissolved organic matter (DOM) concentrations through Hg spike addition analysis. We report a relatively large variation in mass-dependent fractionation (δ^{202}Hg; from −2.12 to −1.32‰) and a smaller, but significant, variation of mass-independent fractionation (Δ^{199}Hg; from −0.35 to −0.12‰) during two years of sampling with streamflow varying from 0.003 to 7.8 L s^{-1}. Large variations in δ^{202}Hg occurred only during low streamflow (<0.6 L s^{-1}), which suggest that under high streamflow conditions a peatland lagg zone between the bog (3.0 ha) and uplands (6.7 ha) becomes the dominant source of Hg in downstream waters. Further, a binary mixing model showed that except for the spring snowmelt period, Hg in streamwater from the catchment was mainly derived from dry deposition of gaseous elemental Hg (73–95%). This study demonstrates the usefulness of Hg isotopes for tracing sources of Hg deposition, which can lead to a better understanding of the biogeochemical cycling and hydrological transport of Hg in headwater catchments.

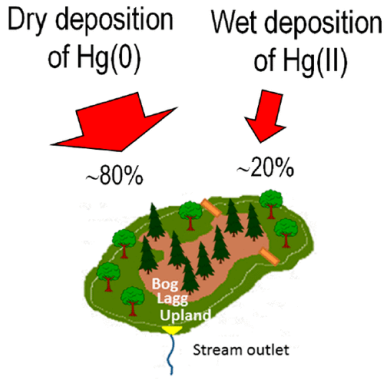

Keywords: Soils | Dissolved organic matter | Deposition | Mercury | Isotopes

Article:

Introduction

Peatlands, a particular type of wetland, store vast amounts of carbon in deep organic soil and are important landscape features in boreal and northern environments.(1) Peatlands are substantial sinks of mercury (Hg) from atmospheric deposition and sources of dissolved organic matter (DOM) and Hg to surface waters.(2, 3) Peatlands are also important sources of methylmercury (MeHg) because saturation at and below peatland water tables maintains anaerobic conditions, under which extensive Hg methylation can occur.(4, 5) Several factors affect how Hg is transported downstream from upland/peatland headwaters. First, DOM movement in flowing water is important because Hg strongly binds with reduced thiol groups on DOM.(6) Second, although peatlands are important areas of Hg cycling and transport, uplands are only intermittent sources of water, DOM, nutrients, and Hg to peatlands.(7) Uplands are sources of water and Hg when shallow subsurface stormflow occurs along lateral flow paths through mineral soils on upland hillslopes.(8) Although couplings between upland and peatland sources and transport processes drive the downstream movement of water, DOM, and Hg, little is known about how atmospheric Hg deposition relates to Hg processing in upland-peatland catchments.(9, 10) In other words, we know little about how various atmospheric Hg sources (either as Hg(0) in dry deposition or as Hg(II) in wet deposition)(11) are directly or indirectly linked to downstream aqueous Hg transport. It is particularly important to differentiate between these two deposition pathways because we currently only monitor wet deposition of Hg through the Mercury Deposition Network of the National Atmospheric Deposition Program (URL: http://nadp.sws.uiuc.edu/mdn).(12) However, recent studies have suggested that dry deposition may be the dominant pathway of Hg deposition in vegetated landscapes.(13-15) Thus, an in-depth understanding of dry deposition will be required to fully understand and predict effects of atmospheric deposition of Hg at landscape and regional scales. Atmospheric Hg may be the substrate for MeHg formation in downstream habitats, and leads to extensive MeHg bioaccumulation and biomagnification in food webs.

New insights into Hg cycling in the environment have been gained through stable Hg isotope studies.(16) Mercury can undergo both mass-dependent fractionation (MDF; expressed as δ^{202}Hg) and mass-independent fractionation (MIF; expressed as Δ^{199}Hg or Δ^{201}Hg), with large-magnitude MIF (>0.4 ‰) of odd-mass isotopes (^{199}Hg and ^{201}Hg) being produced mainly through photoreduction of inorganic Hg and photodegradation of MeHg.(17) Subtle MIF associated with even-mass isotopes (^{200}Hg and ^{204}Hg) has also been recently observed for samples linked to atmospheric origins.(18-20) A number of recent studies have successfully demonstrated that natural-abundance Hg isotopes can help distinguish sources (e.g., natural vs anthropogenic)(20-22) and transformations (e.g., gaseous Hg oxidation; MeHg photodegradation)(23, 24) of Hg in the environment.

A few previous studies have analyzed natural-abundance Hg isotopes in water samples with relatively low DOM levels (such as rain, snow, and lake waters) to examine isotopic variations of Hg in these environmental pools.(13, 18, 19, 21, 25-27) A recent study used ultrafiltration to

collect Hg associated with DOM to measure Hg isotope ratios in streams in a boreal forest catchment where DOM is elevated.(28) This method is feasible but requires large volumes of water (e.g., 50 L) and cumbersome subsequent separation of Hg from DOM and other matrices in the water samples.(28) To make the processing more efficient we validated and used an acidic permanganate/persulfate digestion procedure, used previously for surface water with high solid loads and wastewater samples,(29, 30) and followed by subsequent purge and trap of Hg to transfer it to a small volume of trapping solution.(13, 18, 21) With this approach we removed matrix interferences in water samples (i.e., DOM), which allowed investigation of the isotopic composition of Hg in various Hg source areas (uplands or peatlands) in a well-studied catchment in northern Minnesota. We chose this catchment because previous investigations have provided a foundational knowledge of ecosystem and hydrological processes, and the DOM and Hg source areas and transport are well-known within the watershed.(31-33) Our goal was to examine whether Hg isotopes could be used in peatland catchments to determine the relative importance of different sources of Hg (wet and dry deposition) and elucidate ecosystem processes within the catchment that affect the downstream export of Hg.

Materials and Methods

Study Site and Sample Collection

The study site is a 9.7-ha upland-peatland catchment (S2) in northern Minnesota at the USDA Forest Service's Marcell Experimental Forest (MEF) (see Supporting Information (SI) Figure S1). The 3.2-ha peatland has a central 3.0-ha, ombrotrophic, raised-dome bog with Histosol soil. The bog is surrounded by a 0.2-ha lagg (wet zone on the perimeter of the peatland). There are no inlet streams to the peatland, and the outlet stream originates from the lagg at the area of lowest elevation in the peatland. The bog has a black spruce (*Picea mariana*)-*Sphagnum* community. The uplands have Alfisol soils with a ~0.5 m sandy loam layer overlying a loamy clay aquitard. The upland forest is a stand with mature aspen (*Populus tremuloides*), white birch (*Betula papyrifera*), balsam fir (*Abies balsamea*), and jack pine (*Pinus banksiana*) in the overstory. Meteorological and hydrological data (streamflow, air temperature, and precipitation amount) have been monitored for more than a half century in catchment S2 as part of a long-term research monitoring program.(34) Site information and field measurements are described in detail in SI Part I. We collected streamwater every 2 weeks during 2014 and 2015 at a v-notch weir on the outlet stream of the catchment when the stream flowed (see SI Part II). Streamflow was measured at the v-notch weir, and we apportioned streamflow into slow flow and quick flow components.(35) We consider quick flow to be streamflow that occurs in response to a rainfall or snowmelt event. Occasionally, we collected upland runoff samples (that included upland runoff above frozen soils and near surface flow through the forest floor) and subsurface stormflow samples as well as porewater samples at the lagg. In spring 2015, we collected soil samples (50 cm long cores of bog, lagg and upland soils) and vegetation samples (needles of black spruce (bog), grass litter of *Eriophorum* spp., needles of tamarack (bog), and leaf litter (aspen and white birch)) to represent different Hg sources that may have affected stream Hg concentrations and isotopic compositions. All samples were shipped on ice overnight to the analytical laboratory at the University of North Carolina at Greensboro and refrigerated or frozen until processed.

Sample Processing and Analyses

Two bottles of streamwater were collected at each sampling time for general water chemistry (cations and total organic carbon (TOC) in an HDPE bottle) and both Hg concentration (total-Hg and MeHg) and Hg isotopic analyses (in an acid-cleaned 2 L Teflon bottle). Soil and vegetation samples were collected, acid-digested, and analyzed for total-Hg (see SI Part III). Recent sampling and analyses of streamwater have shown TOC and DOC to be equivalent measurements for stream, porewater, and upland runoff water samples from the S2 catchment.(36) Herein, we report TOC, as that is what we actually measured, but we consider TOC and dissolved organic carbon (DOC) concentrations to be equivalent.

Since many of the water samples (except upland runoff and subsurface flow) had high TOC concentrations (range for all aqueous samples: 8–116 mg L^{-1}), we added an acidic mixture of permanganate and persulfate to the aqueous samples in the Teflon bottle. Per 1 L of water samples, we added 10 mL of acidic digestant (20 HNO_3:1 H_2SO_4) and 10 mL of oxidizing reagents (5% (w/v) of $KMnO_4$ and 2.5% (w/v) of $K_2S_2O_8$ dissolved in high-purity water) followed by heating in an oven at 95 °C overnight,(29, 30) which has been previously shown to result in full recovery of Hg from water samples with very high TOC and/or high suspended solid concentrations. We compared this method with the traditional method of BrCl oxidation of water samples followed by complete UV oxidation,(37) which we assumed to result in complete breakdown of DOM and Hg and which should result in Hg not being associated with any binding sites after the treatment (see SI Part IV). The use of UV oxidization is known to be much more effective in completely breaking down organic matter than adding BrCl alone, but we were concerned that UV photochemical reactions might fractionate Hg isotopes in the samples.(38) We determined that the acidic permanganate and persulfate approach released >92% of Hg from water samples. Standard addition analyses of the digested samples led to an average of 99.5% recovery of Hg (SI Table S1).

To collect Hg from aqueous samples for isotopic measurements, we used a purge and trap setup to extract Hg from each ∼1 L of fully digested and neutralized water sample by continuous $SnCl_2$ reduction, and we concentrated the released Hg into a small trap (6–7 g) solution of 1% $KMnO_4$ in 10% H_2SO_4 solution over 3–4 h (see detailed procedures in SI Part V and illustrated setup in Figure S2). For solid samples, we combusted the homogenized samples in a two-stage furnace over 6 h with subsequent sample matrix removal and concentration of Hg into a final 1% $KMnO_4$ trap solution (see SI Part V). All final sample solutions were measured for total-Hg content, and the concentrations were adjusted to match within 5% the concentration of the isotopic bracketing standard (SRM NIST-3133). Mercury isotope ratios of samples were analyzed using a multicollector-inductively coupled plasma-mass spectrometer (MC-ICP-MS) (see SI Part VI) at the Biogeochemistry and Environmental Isotope Geochemistry Laboratory, University of Michigan (Ann Arbor, MI).

Quality Control and Data Analyses

Quality control and assurance for Hg isotopic analysis were performed through analyzing a secondary isotope standard solution throughout the study (UM-Almadén), and spiking of a Hg isotope standard (NIST-3133) through the entire sample processing procedure for water sample analysis, as well as analyses of standard reference materials of solid samples, that is, SRM NIST-

1515 (Apple Leaves) and SRM MESS-3 (Marine Sediment). Detailed information can be found in SI Part V and Part VI, and isotopic results for solid SRMs are summarized in SI Table S2. Linear regression analyses were performed using SigmaPlot 12.5 (Systat) and the significance level for all statistical analyses was $\alpha = 0.05$.

Results and Discussion

Streamflow and Mercury Levels

Streamflow was highly variable within and between the two years of the study. The largest amounts of stormflow occurred during late spring and summer in 2014, and during spring, fall and early winter in 2015 (SI Figure S3). Snowmelt during spring is typically a period of extended high flow, and often includes the largest flow event of the year.(7, 31) However, during the winter of 2014/2015 there was little snowfall leading to much less snowmelt and streamflow during late winter and early spring of 2015 (SI Figure S3).

Over the two years of study, we collected 24 streamwater samples (2 L each, $n = 12$ per year) under variable streamflow from 0.003 to 7.8 L s^{-1} (SI Table S4). Concentrations of TOC varied from 37 to 116 mg L^{-1}, (unfiltered) total-Hg varied from 4.6 to 25.0 ng L^{-1}, and (unfiltered) MeHg varied from <0.04 to 1.47 ng L^{-1} (SI Table S4). In contrast to many other stream studies,(3, 39, 40) we did not observe a significant relationship between TOC and total-Hg or MeHg among the stream samples ($p > 0.05$). We also combined total-Hg, MeHg, and %MeHg data from our study with previously published studies at the S2 catchment during 1993, 1994, 1995, and 2005 (SI Figure S4).(41, 42) We observed a weak positive correlation ($r^2 = 0.03$; $p = 0.07$) between $\log_{10}$-transformed total-Hg and $\log_{10}$-transformed streamflow. Interestingly, both $\log_{10}$-transformed MeHg and $\log_{10}$-transformed %MeHg exponentially decreased (both $p < 0.0001$) with $\log_{10}$-transformed streamflow, showing streamwater MeHg concentrations were highest when flow declined in this small upland-peatland catchment. The results are within our expectations because as streamflow increases we expect to see more upland runoff with lower MeHg levels, and this increased upland runoff should contribute a higher fraction of water to streamflow. Thus, a dilution effect occurred when MeHg in water from the bog was mixed with upland runoff.

In addition to stream waters, we also analyzed other water types including upland runoff ($n = 2$) and subsurface stormflow through upland soils ($n = 3$), as well as lagg porewater ($n = 2$) (SI Table S6). Upland runoff samples had higher total-Hg (18.3–56.8 ng L^{-1}) but lower MeHg (0.04–0.06 ng L^{-1}) relative to other sample types, whereas lagg porewater samples had the lowest total-Hg (10.4–13.1 ng L^{-1}), but with the highest MeHg (0.27–0.33 ng L^{-1}) and %MeHg (2.1–3.2%). These results are consistent with previous findings that the lagg is a hotspot of microbial Hg methylation in this catchment.(5)

Stable Mercury Isotopes

As shown in Figure 1A, the lagg core had the highest total-Hg concentrations (108–222 ng/g, $n = 10$), with less in the peat (bog) core (34–133 ng/g, $n = 10$), and much less in the upland soil (5.6–92 ng/g, $n = 5$) (SI Table S3), which consists of mineral soil except for the higher total-Hg

concentrations in the top 5–10 cm of the forest floor. All three cores had a narrow range of δ^{202}Hg (MDF) values (from −1.60 to −1.30 ‰) at the bottom (30–50 cm), but we found a wider range in δ^{202}Hg in the top 20 cm of the cores (from −2.30 to −1.30‰); the δ^{202}Hg value was highest in the top 20 cm of upland soil core (−1.48 to −1.35‰), lowest in the top 20 cm of peat core (−2.24 to −2.06‰), and intermediate in the top 20 cm of lagg core (−1.88‰) (Figure 1B; SI Table S3). It is noteworthy that the top 20 cm of the upland soil had the highest Δ^{199}Hg (MIF) values (−0.25 to −0.10‰) while the top 20 cm of the peat core (−0.36 to −0.31‰) and lagg core (−0.39‰) both had slightly lower Δ^{199}Hg (MIF) values (Figure 1C; SI Table S3). Nevertheless, the differences in Δ^{199}Hg values were relatively small compared to δ^{202}Hg values. These Hg isotope results for the cores also suggest that geogenic sources of Hg, which have near-zero Δ^{199}Hg (MIF) values,(16, 43) are not a dominant source of Hg in these soils. The top layers of the upland soil core had the highest Δ^{199}Hg (closest to zero; Figure 1C) but we speculate that this may be due to the relatively higher inputs of Hg from wet deposition (precipitation) (see below).

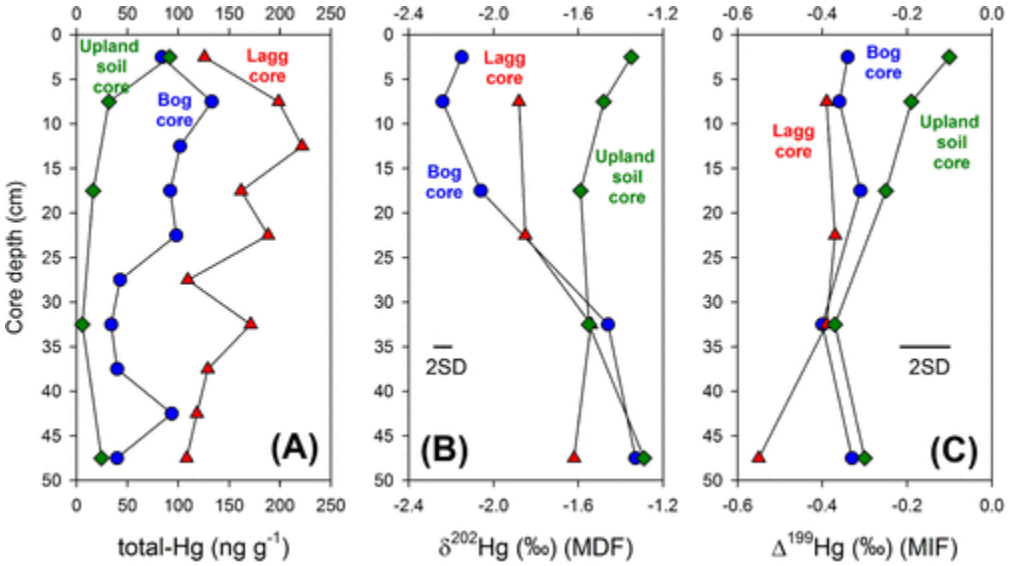

Figure 1. (A) Total-mercury concentrations (total-Hg), (B) mass-dependent fractionation (MDF; as δ^{202}Hg) and (C) mass-independent fractionation (MIF; as Δ^{199}Hg) of 50 cm cores collected at the peatland, lagg and upland forest in April, 2015. Only selected layers (4–5 per core) were analyzed for stable mercury isotopes. For (B) and (C), error bars represent external analytical reproducibility (2 SD) of our isotope measurements.

Overall, there were relatively large ranges in Hg isotopic composition among streamwater samples, with δ^{202}Hg ranging from −2.12 to −1.32 ‰ and Δ^{199}Hg ranging from −0.35 to −0.12 ‰ over the two years of sampling (Figure 2 and SI Table S4). The lowest values of both δ^{202}Hg and Δ^{199}Hg in streamwater samples were similar to surficial peat (top 20 cm of core) while the highest values of both δ^{202}Hg and Δ^{199}Hg for water samples were similar to surficial upland soil (top 20 cm of core) (Figure 2). Surface lagg cores had δ^{202}Hg values similar to many water samples but their Δ^{199}Hg values were slightly lower than water samples, although the differences were within the analytical uncertainty (2SD) (Figure 2). As expected, isotopic compositions of Hg in vegetation samples collected in upland and peatland areas (δ^{202}Hg: −2.37 to −2.17 ‰; Δ^{199}Hg: −0.48 to −0.24 ‰; n = 4) (SI Table S5) were also similar to those collected elsewhere in North America, e.g., Wisconsin (δ^{202}Hg: −2.53 to −1.79 ‰; Δ^{199}Hg: −0.40 to −0.23 ‰; n =

18)(13) and across multiple forests (δ^{202}Hg: −2.67 to −2.08 ‰; Δ^{199}Hg: −0.47 to −0.06 ‰; n = 84).(44) The δ^{202}Hg values of vegetation were among the lowest values we observed in all samples collected from the S2 catchment (Figure 2).

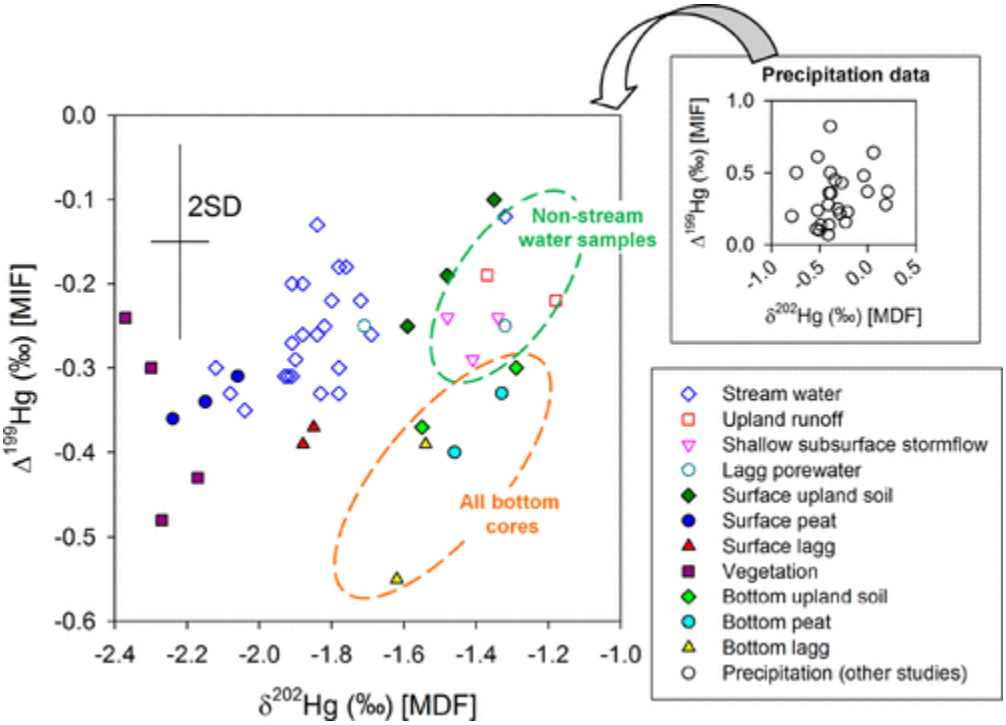

Figure 2. Stable Hg isotope compositions of all samples in this study, showing mass-dependent fractionation (MDF; as δ^{202}Hg) and mass-independent fractionation (MIF; as Δ^{199}Hg); the inset shows isotopic data of Hg in previous precipitation studies in the Great Lakes region.(13, 18) Error bars show typical external analytical reproducibility (2SD) of our stable Hg isotope measurements in this study.

For nonstreamwater samples collected within the catchment (i.e., upland runoff, subsurface stormflow, and porewater at the lagg), δ^{202}Hg values were mostly higher than streamwater samples while their Δ^{199}Hg values were also near the high range of streamwater samples (Figure 2; SI Table S4 and SI Table S6). It is interesting to note that these nonstreamwater samples had a smaller range of both δ^{202}Hg and Δ^{199}Hg values (δ^{202}Hg: −1.71 to −1.18‰; Δ^{199}Hg: −0.29 to −0.19‰) than streamwater samples, suggesting that Hg in lagg porewater was derived from the upland through subsurface stormflow, since there were no significant differences in Hg isotopic compositions (both δ^{202}Hg and Δ^{199}Hg) between the top 20 cm of the upland soil core and the lagg porewater samples ($p > 0.05$). Moreover, we found that the δ^{202}Hg values, but not Δ^{199}Hg values, matched well between these nonstreamwater samples and the bottom sections of all three soil cores we collected (Figure 1 and Figure 2).

Isotopic Variations with Streamflow and Mixing Model Calculation

Among the streamwater samples we found that streamflow strongly influenced both δ^{202}Hg and Δ^{199}Hg values (Figure 3A and B). We can group the isotopic data into “low streamflow” (<0.6 L s^{-1}) and “high streamflow” (2.2–7.8 L s^{-1}), and most of the variations in δ^{202}Hg and Δ^{199}Hg

values were found in samples grouped as low streamflow. However, it should be noted that even during low streamflow there may have been some "quick flow" from saturated areas of the peatland that allowed event waters to be rapidly transmitted to the stream (SI Table S4). During high streamflow conditions there was only a narrow range of δ^{202}Hg (mean ± S.D.: −1.86 ± 0.05 ‰; n = 8) and Δ^{199}Hg (mean ± S.D.: −0.27 ± 0.06 ‰; n = 8), with one obvious outlier for Δ^{199}Hg under high streamflow (Figure 3B).

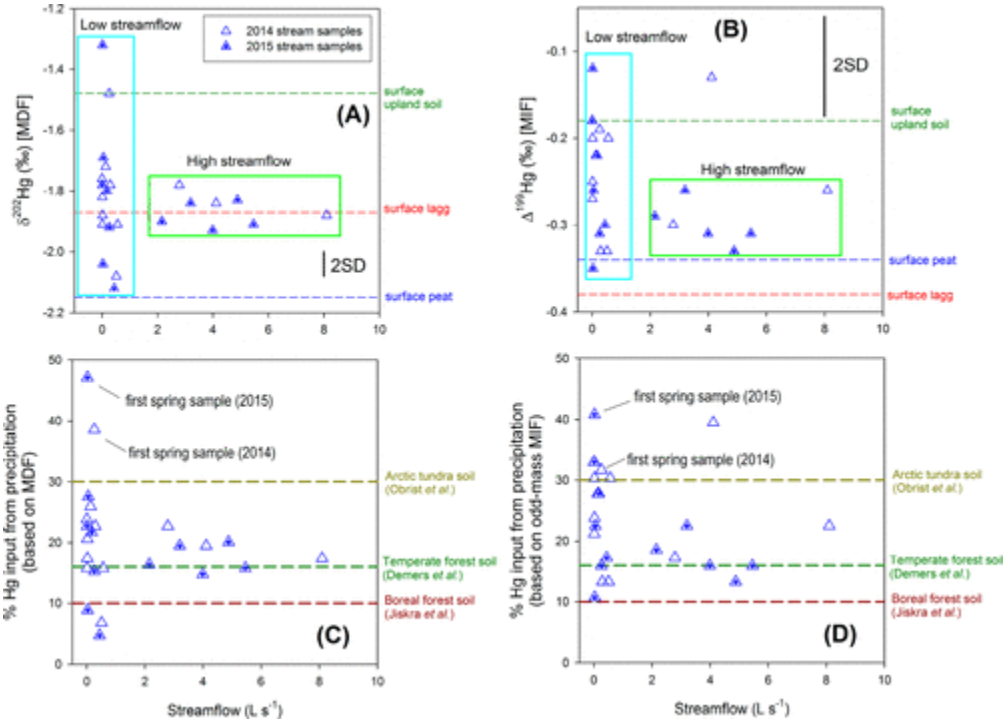

Figure 3. (A) Mass-dependent fractionation (MDF; as δ^{202}Hg) and (B) mass-independent fractionation (MIF; as Δ^{199}Hg) of Hg in streamwater as a function of streamflow at the S2 catchment; for (A) and (B), horizontal dashed lines represent the mean values in the top layer (0–20 cm) of different cores collected; error bars represent external analytical reproducibility (2 SD) of our isotopic measurements. Results of binary mixing model estimating the percent Hg contributed from wet deposition to Hg in streamwater at the S2 catchment based on (C) MDF; as δ^{202}Hg, and (D) odd-mass MIF; as Δ^{199}Hg.; horizontal dashed lines indicate the average percentage contribution of wet deposition to Hg deposition in different landscape types.(13-15)

Stream water samples with the lowest δ^{202}Hg values only occurred when streamflow was entirely slow flow (i.e., there was no quick flow, SI Table 2) and during which all the water in the stream originated from the peatland (SI Figure S5). We also note that streamwater samples with higher δ^{202}Hg values only occurred when there was quick flow (>0%), showing a streamflow response to upland sources and/or precipitation (e.g., snow) events. Alternatively, in situ Hg transformations such as photoreduction of Hg(II) may become more important and shift both MDF and MIF signatures during the lowest of streamflows when the residence time of water in the channel may be substantially increased.

It has been found that Hg accumulated in foliage as a result of dry deposition of Hg(0) has much lower δ^{202}Hg and slightly lower Δ^{199}Hg value(13, 44) than aqueous Hg found in wet

deposition.(13, 18, 19, 21) This isotopic contrast has allowed the quantification of the proportion of Hg derived from dry deposition (as elemental Hg) vs wet deposition (as oxidized Hg) in different ecosystems by analyzing Hg isotopes in forest floor or vegetation substrates.(13-15, 45) Following this approach, we estimated the percent contribution of dry vs wet deposition to Hg in streamwater collected at the outlet of the S2 catchment using a binary mixing model. Since there is a much wider range of δ^{202}Hg than Δ^{199}Hg values, we first use MDF values for the mixing model because it provides better accuracy for the model output (i.e., %Hg from wet deposition). For the dry deposition endmember, we used the average δ^{202}Hg value of foliage samples in the S2 catchment (mean ± S.D.: δ^{202}Hg: −2.19 ± 0.15‰; n = 4). For the wet deposition endmember, we used the average δ^{202}Hg values in precipitation samples from the Great Lakes region published previously (mean ± S.D.: −0.32 ± 0.25‰; n = 25).(13, 18, 26)

One common consideration when using precipitation Hg isotope data is that aqueous Hg would likely be adsorbed to particles (e.g., organic matter, soil minerals) before being exported as streamflow.(6, 46) A previous Hg isotope study used an average MDF shift due to adsorption of −0.4‰ to account for the inputs of precipitation Hg into the water column and binding to particles in the Great Lakes.(20) However, in our study catchment if precipitation Hg directly contributes to Hg in streamflow, then it is likely that most, if not all, precipitation Hg would quickly bind to DOM in the surface water within the peatland, and thus this would cause negligible or no MDF of Hg isotopes. This presumption is supported by a recent field study demonstrating no significant MDF of Hg isotopes between bulk soil and surface water samples in a boreal forest ecosystem,(28) implying that Hg desorbed from soil or decomposed litter may still be well bound to DOM. Therefore, these results imply that in this situation we may directly compare Hg isotope ratios in streamwater with those in bulk materials (e.g., foliage and soil) without considering secondary processes, that is, a shift of δ^{202}Hg.(28)

From our mixing calculation based on MDF values in stream samples we found an average of 18 ± 3% (±SD; n = 8) of wet deposition contributing to streamwater Hg under high streamflow conditions, and from ∼5% to ∼47% of wet deposition contributing to streamwater Hg under low streamflow conditions (Figure 3C). Second, we used odd-mass MIF values (Δ^{199}Hg) for the binary mixing models as MIF can be advantageous because it is not influenced by nonphotochemical processes such as adsorption to particles.(17) We obtained a similar estimate if our mixing model was based on Δ^{199}Hg values (Figure 3D). Although they do not follow one another exactly, the two estimation methods (based on δ^{202}Hg vs Δ^{199}Hg) yielded reasonable agreement with each other (SI Figure S6); it should be noted that the smaller range of odd-mass MIF values in streamwater samples may imply lower resolution and power in estimation of Hg input from precipitation. However, even-mass MIF values (Δ^{200}Hg and Δ^{204}Hg) were not observed to have a large enough magnitude (e.g., > 0.20 ‰) to show variation that might be related to sample types (refer to SI Tables S3, S4, S5, and S6). We note that while Δ^{204}Hg is generally negative in precipitation, Δ^{204}Hg in Hg(0) has been shown to be slightly positive.(13, 47) Therefore, in mixtures of Hg deposited as both wet and dry deposition the even-mass MIF signal can be canceled out, especially if dry deposition is greater than wet deposition inputs as we have found to be the case in this study. Notably, the two stream samples with the highest % Hg contribution from wet deposition were each the first spring samples collected during low streamflow conditions. At those times, streamwater and Hg originated from snowmelt directly to the stream at a time when the (frozen) bog was not yet contributing water to the stream. These

data, along with a few recent studies analyzing Hg isotopes in soils or vegetation samples,(13-15, 45) demonstrate the importance and dominance of dry deposition (i.e., foliage uptake of Hg) to Hg accumulation in forested ecosystems and to the ultimate export of Hg to aquatic ecosystems. These results are in contrast to earlier studies using Hg concentration analyses alone, that suggested much higher proportions of Hg accumulation in forests due to wet deposition.(3, 48) Atmospheric Hg deposition is most widely and consistently measured in the USA by the Mercury Deposition Network (URL: http://nadp.sws.uiuc.edu/mdn), including the MN16 MDN site at the MEF. This network measures Hg in wet precipitation (rain and snow) but not dry deposition. With recent studies showing that dry deposition of Hg(0) is a dominant process of Hg deposition in forested watersheds, we presume that our general knowledge of Hg deposition as based on wet deposition monitoring represents a systematic bias toward underestimation of Hg deposition in forested landscapes. Additional work will be needed to quantify dry deposition of Hg on regional scales, in addition to wet deposition.

Our current results also raise an important question regarding the ultimate fate of Hg from wet deposition. It is possible that this pool of aqueous Hg could be more susceptible to photoreduction and could be volatilized as gaseous elemental Hg back to the atmosphere. Alternatively, it is possible that this pool of aqueous Hg is more readily methylated than Hg that is dry deposited to foliage.(9) Additional research will be needed to resolve these complexities.

Interpretation of Results in the Context of Catchment Hydrology

We interpret the data presented here within the well-established hydrological setting of this headwater peatland catchment. Laggs occur at a landscape position that receives runoff from the central raised-dome bog and the surrounding forest uplands. The lagg yields water to the outlet stream whenever there is streamflow.(7, 31) In contrast, uplands intermittently yield water to the lagg and stream, but only during the wettest conditions, when upland soils become saturated and water flows laterally downslope as subsurface stormflow.(49) Upland runoff does occasionally occur on upland hillslopes, but it is quantitatively unimportant relative to the effects of subsurface stormflow on seasonal or annual TOC yields.(2, 7, 31) The high total-Hg content and intermediate δ^{202}Hg values of lagg peat shows the lagg to be a zone where Hg from upland subsurface stormflow accumulates on organic matter. The correspondence of δ^{202}Hg values between streamwater and surface (0–20 cm) lagg peat shows that the majority of Hg in streamwater is derived from the lagg zone, which itself is a mixture of Hg from the bog and uplands during high streamflow. We also examined whether the variation in δ^{202}Hg values for low flow samples was related to redox sensitive elements such as iron (Fe), but we did not find a significant relationship between total Fe and δ^{202}Hg values of Hg in streamwater (SI Figure S7).

The lagg, despite its small area (0.2 ha) compared to the bog (3.0 ha), has been identified as a hydrological and biogeochemical hotspot in this and other peatland catchments at the MEF.(5, 7, 32) Our Hg isotope data corroborate that perspective and suggest that the lagg was most crucial in determining the stream Hg isotopic composition as the lagg zone is the most proximal hydrological connection to the stream outlet and is consequently biogeochemically important as a hotspot that affects stream chemistry (SI Figure S1). In most cases, especially during stormflow, the isotopic composition of Hg in stream waters resembled those of surface (0–20 cm) lagg peat. However, since the surface upland soil and bog peat had a Hg isotopic

composition at the opposite end of the range of δ^{202}Hg values, simple mixing of Hg from these two sources(41) could also produce the δ^{202}Hg values of Hg isotopes that we observed in stream waters (Figure 1B). Another important caveat of the data interpretation is that Hg derived from precipitation could potentially be mixed with surface upland soil, and thus stream Hg isotope compositions (MDF and MIF) may reflect inputs from both upland soil (derived from previous precipitation and dry deposition) and recent precipitation, which we are unable to apportion in streamwater based on our current data set.

Overall, this study demonstrates the versatility of stable Hg isotopes for revealing how sources, transport processes, and biogeochemical transformations affect the variation of streamwater Hg over time in this small peatland/upland catchment. Using acidic permanganate/persulfate chemical digestion of waters to eliminate possible interferences from high DOM concentrations and followed by purge and trap pre-enrichment of Hg, it was feasible to determine the natural-abundance isotopic compositions of dissolved and/or particulate Hg in peatland ecosystems. This approach is especially important because headwater peatlands are widespread in northern latitudes, crucial atmospheric sinks of Hg, hotspots of MeHg production, and sources of downstream DOM, inorganic Hg and MeHg. Our results provide insight into the interplay and effects of distinct source areas on stream Hg dynamics beyond previous Hg studies in this catchment.(2, 3, 5, 8, 41, 42) Our results also demonstrate the dominant role of dry deposition in Hg accumulation in forests and Hg export via streamflow.

Acknowledgment

This study was partially supported by a National Science Foundation award to M.T.K.T. and J.D.B. (DEB-1354811 and DEB-1353850), University of North Carolina at Greensboro to G.E.W. and M.T.K.T., and China Scholarship Council to X.N. Special thanks go to M. Johnson (University of Michigan) for his expert assistance with mercury isotope analysis and his help verifying mercury recovery during digestion method comparisons. We greatly appreciate B. Munson and L. Mielke (USDA Forest Service) who collected many water samples, and J. Larson (USDA Forest Service) who analyzed general water chemistry. Their contributions, with those of S.D. Sebestyen and R.K. Kolka, and chemical analyses were funded by the Northern Research Station of USDA Forest Service. The research was partially funded by the USDA Forest Service and this manuscript has been coauthored by Federal employees. The United States Government retains and the publisher, by accepting the article for publication, acknowledges that the United States Government retains a nonexclusive, paid-up, irrevocable, worldwide license to publish or reproduce the published form of this manuscript, or allow others to do so, for United States Government purposes.

References

1. Gorham, E. Northern peatlands: Role in the carbon cycle and probable responses to climatic warming Ecol. Appl. **1991**, 1, 182– 195 DOI: 10.2307/1941811 Google Scholar
2. Kolka, R. K.; Nater, E. A.; Grigal, D. F.; Verry, E. S. Atmospheric inputs of mercury and organic carbon into a forested upland bog watershed Water, Air, Soil Pollut. **1999**, 113, 273– 294 DOI: 10.1023/A:1005020326683 Google Scholar

3. Grigal, D. F.; Kolka, R. K.; Fleck, J. A.; Nater, E. A. Mercury budget of an upland-peatland watershed Biogeochemistry **2000**, 50, 95– 109 DOI: 10.1023/A:1006322705566 Google Scholar

4. Branfireun, B. A.; Roulet, N. T.; Kelly, C. A.; Rudd, J. W. M. In situ sulphate stimulation of mercury methylation in a boreal peatland: Toward a link between acid rain and methylmercury contamination in remote environments Global Biogeochem. Cy. **1999**, 13, 743– 750 DOI: 10.1029/1999GB900033 Google Scholar

5. Mitchell, C. P. J.; Branfireun, B. A.; Kolka, R. K. Spatial characteristics of net methylmercury production hot spots in peatlands Environ. Sci. Technol. **2008**, 42, 1010– 1016 DOI: 10.1021/es0704986 Google Scholar

6. Ravichandran, M. Interactions between mercury and dissolved organic matter – A review Chemosphere **2004**, 55, 319– 331 DOI: 10.1016/j.chemosphere.2003.11.011 Google Scholar

7. Verry, E. S.; Brooks, K. N.; Nichols, D. S.; Ferris, D. R.; Sebestyen, S. D. Watershed hydrology. In Peatland Biogeochemistry and Watershed Hydrology at the Marcell Experimental Forest; Kolka, R. K.; Sebestyen, S. D.; Verry, E. S.; Brooks, K. N., Eds.; CRC Press: Boca Raton, FL, 2011. Google Scholar

8. Mitchell, C. P. J.; Branfireun, B. A.; Kolka, R. K. Methylmercury dynamics at the upland-peatland interface: Topographic and hydrogeochemical controls Water Resour. Res. **2009**, 45, W02406 DOI: 10.1029/2008WR006832 Google Scholar

9. Hintelmann, H.; Harris, R.; Heyes, A.; Hurley, J. P.; Kelly, C. A.; Krabbenhoft, D. P.; Lindberg, S.; Rudd, J. W. M.; Scott, K. J.; St.Louis, V. L. Reactivity and mobility of new and old mercury deposition in a boreal forest ecosystem during the first year of the METAALICUS study Environ. Sci. Technol. **2002**, 36, 5034– 5040 DOI: 10.1021/es025572t Google Scholar

10. Oswald, C. J.; Heyes, A.; Branfireun, B. A. Fate and transport of ambient mercury and applied mercury isotope in terrestrial upland soils: insights from the METAALICUS watershed Environ. Sci. Technol. **2014**, 48, 1023– 1031 DOI: 10.1021/es404260f Google Scholar

11. Lindberg, S. E.; Stratton, W. J. Atmospheric mercury speciation: Concentrations and behavior of reactive gaseous mercury in ambient air Environ. Sci. Technol. **1998**, 32, 49– 57 DOI: 10.1021/es970546u Google Scholar

12. Prestbo, E. M.; Gay, D. A. Wet deposition of mercury in the U.S. and Canada, 1996–2005: Results and analysis of the NADP mercury deposition network (MDN) Atmos. Environ. **2009**, 43, 4223– 4233 DOI: 10.1016/j.atmosenv.2009.05.028 Google Scholar

13. Demers, J. D.; Blum, J. D.; Zak, D. R. Mercury isotopes in a forested ecosystem: Implications for air-surface exchange dynamics and the global mercury cycle Glob. Biogeochem. Cycles **2013**, 27, 222– 238 DOI: 10.1002/gbc.20021 Google Scholar

14. Jiskra, M.; Wiederhold, J. G.; Skyllberg, U.; Kronberg, R.-M.; Hajdas, I.; Kretzschmar, R. Mercury deposition and re-emission pathways in boreal forest soils investigated with Hg

isotope signatures Environ. Sci. Technol. **2015**, 49, 7188– 7196 DOI: 10.1021/acs.est.5b00742 Google Scholar

15. Obrist, D.; Agnan, Y.; Jiskra, M.; Olson, C. L.; Colegrove, D. P.; Hueber, J.; Moore, C. W.; Sonke, J. E.; Helmig, D. Tundra uptake of atmospheric elemental mercury drives Arctic mercury pollution Nature **2017**, 547, 201– 204 DOI: 10.1038/nature22997 Google Scholar
16. Blum, J. D. Applications of stable mercury isotopes to biogeochemistry. In Handbook of Environmental Isotope Geochemistry; Baskaran, M., Ed.; Springer: Heidelberg, Germany, 2011; pp 229– 245. Google Scholar
17. Bergquist, B. A.; Blum, J. D. Mass-dependent and -independent fractionation of Hg isotopes by photoreduction in aquatic systems Science **2007**, 318, 417– 420 DOI: 10.1126/science.1148050 Google Scholar
18. Gratz, L. E.; Keeler, G. J.; Blum, J. D.; Sherman, L. S. Isotopic composition and fractionation of mercury in Great Lakes precipitation and ambient air Environ. Sci. Technol. **2010**, 44, 7764– 7770 DOI: 10.1021/es100383w Google Scholar
19. Chen, J.; Hintelmann, H.; Feng, X.; Dimock, B. Unusual fractionation of both odd and even mercury isotopes in precipitation from Peterborough, ON, Canada Geochim. Cosmochim. Acta **2012**, 90, 33– 46 DOI: 10.1016/j.gca.2012.05.005 Google Scholar
20. Lepak, R. F.; Yin, R.; Krabbenhoft, D. P.; Ogorek, J. M.; DeWild, J. F.; Holsen, T. M.; Hurley, J. P. Use of stable isotope signatures to determine mercury sources in the Great Lakes Environ. Sci. Technol. Lett. **2015**, 2, 335– 341 DOI: 10.1021/acs.estlett.5b00277 Google Scholar
21. Sherman, L. S.; Blum, J. D.; Keeler, G. J.; Demers, J. D.; Dvonch, J. T. Investigation of local mercury deposition from a coal-fired power plant using mercury isotopes Environ. Sci. Technol. **2012**, 46, 382– 390 DOI: 10.1021/es202793c Google Scholar
22. Wiederhold, J. G.; Skyllberg, U.; Drott, A.; Jiskra, M.; Jonsson, S.; Björn, E.; Bourdon, B.; Kretzschmar, R. Mercury isotope signatures in contaminated sediments as a tracer for local industrial pollution sources Environ. Sci. Technol. **2015**, 49, 177– 185 DOI: 10.1021/es5044358 Google Scholar
23. Sun, G.; Sommar, J.; Feng, X.; Lin, C. J.; Ge, M.; Wang, W.; Yin, R.; Fu, X.; Shang, L. Mass-dependent and-independent fractionation of mercury isotope during gas-phase oxidation of elemental mercury vapor by atomic Cl and Br. Environ. Sci. Technol. **2016**, 50, 9232– 9241 DOI: 10.1021/acs.est.6b01668 Google Scholar
24. Tsui, M. T. K.; Blum, J. D.; Kwon, S. Y.; Finlay, J. C.; Balogh, S. J.; Nollet, Y. H. Photodegradation of methylmercury in stream ecosystems Limnol. Oceanogr. **2013**, 58, 13– 22 DOI: 10.4319/lo.2013.58.1.0013 Google Scholar
25. Sherman, L. S.; Blum, J. D.; Johnson, K. P.; Keeler, G. J.; Barres, J. A.; Douglas, T. A. Mass-independent fractionation of mercury isotopes in Arctic snow driven by sunlight Nat. Geosci. **2010**, 3, 173– 177 DOI: 10.1038/ngeo758 Google Scholar

26. Sherman, L. S.; Blum, J. D.; Dvonch, J. T.; Gratz, L. E.; Landis, M. S. The use of Pb, Sr, and Hg isotopes in Great Lakes precipitation as a tool for pollution source attribution Sci. Total Environ. **2015**, 502, 362– 374 DOI: 10.1016/j.scitotenv.2014.09.034 Google Scholar

27. Chen, J.; Hintelmann, H.; Zheng, W.; Feng, X.; Cai, H.; Wang, Z.; Yuan, S.; Wang, Z. Isotopic evidence for distinct sources of mercury in lake waters and sediments Chem. Geol. **2016**, 426, 33– 44 DOI: 10.1016/j.chemgeo.2016.01.030 Google Scholar

28. Jiskra, M.; Wiederhold, J.; Skyllberg, U.; Kronberg, R.-M.; Kretzschmar, R. Source tracing of natural organic matter bound mercury in boreal forest runoff with mercury stable isotopes Environ. Sci. Process. Impacts **2017**, 19, 1235– 1248 DOI: 10.1039/C7EM00245A Google Scholar

29. Balogh, S. J.; Meyer, M. L.; Johnson, D. K. Mercury and suspended sediment loadings in the lower Minnesota River Environ. Sci. Technol. **1997**, 31, 198– 202 DOI: 10.1021/es960327t Google Scholar

30. Balogh, S. J.; Nollet, Y. H. Mercury mass balance at a wastewater treatment plant employing sludge incineration with offgas mercury control Sci. Total Environ. **2008**, 389, 125– 131 DOI: 10.1016/j.scitotenv.2007.08.021 Google Scholar

31. Verry, E. S.; Janssens, J. Geology, vegetation, and hydrology of the S2 bog at the MEF: 12,000 years in northern Minnesota. In Peatland Biogeochemistry and Watershed Hydrology at the Marcell Experimental Forest; Kolka, R. K.; Sebestyen, S. D.; Verry, E. S.; Brooks, K. N., Eds.; CRC Press: Boca Raton, FL, 2011. Google Scholar

32. Urban, N.; Verry, E. S.; Eisenreich, S.; Grigal, D. F.; Sebestyen, S. D. Element cycling in upland/ peatland watersheds. In Peatland Biogeochemistry and Watershed Hydrology at the Marcell Experimental Forest; Kolka, R. K.; Sebestyen, S. D.; Verry, E. S.; Brooks, K. N., Eds.; CRC Press: Boca Raton, FL, 2011. Google Scholar

33. Kolka, R. K.; Mitchell, C. P. J.; Jeremiason, J. D.; Hines, N. A.; Grigal, D. F.; Engstrom, D. R.; Coleman-Wasik, J. K.; Nater, E. A.; Johnson, B.; Almendinger, J. E.; Branfireun, B.; Brezonik, P. L.; Cotner, J. B. Mercury cycling in peatland watersheds. In Peatland Biogeochemistry and Watershed Hydrology at the Marcell Experimental Forest; Kolka, R. K.; Sebestyen, S. D.; Verry, E. S.; Brooks, K. N., Eds.; CRC Press: Boca Raton, FL, 2011. Google Scholar

34. Sebestyen, S. D.; Dorrance, C.; Olson, D. M.; Verry, E. S.; Kolka, R. K.; Elling, A. E.; Kyllander, R. Long-term monitoring sites and trends at the Marcell Experimental Forest. In Peatland Biogeochemistry and Watershed Hydrology at the Marcell Experimental Forest; Kolka, R. K.; Sebestyen, S. D.; Verry, E. S.; Brooks, K. N., Eds.; CRC Press: Boca Raton, FL, 2011. Google Scholar

35. Nathan, R. J.; McMahon, T. A. Evaluation of automated techniques for base flow and recession analyses Water Resour. Res. **1990**, 26, 1465– 1473 DOI: 10.1029/WR026i007p01465 Google Scholar

36. Sebestyen, S. D.; Funke, M. M.; Cotner, J. B.; Larson, J. B.; Aspelin, N. A. Water Chemistry Data for Studies of the Biodegradability of Dissolved Organic Matter in Peatland Catchments

at the Marcell Experimental Forest: 2009 to 2011. Forest Service Research Data Archive, Fort Collins, CO. DOI: 10.2737/RDS-2017-0067 . Google Scholar

37. USEPA. Guidance for Implementation and Use of EPA Method 1631 for the Determination of Low-Level Mercury (40 CFR part 136); United States Environmental Protection Agency, Office of Water: Washington, DC, 2001. Google Scholar

38. Mead, C.; Lyons, J. R.; Johnson, T. M.; Anbar, A. D. Unique Hg stable isotope signatures of compact fluorescent lamp-sourced Hg Environ. Sci. Technol. **2013**, 47, 2542– 2547 DOI: 10.1021/es303940p Google Scholar

39. Brigham, M. E.; Wentz, D. A.; Aiken, G. R.; Krabbenhoft, D. P. Mercury cycling in stream ecosystems. 1. Water column chemistry and transport Environ. Sci. Technol. **2009**, 43, 2720– 2725 DOI: 10.1021/es802694n Google Scholar

40. Tsui, M. T. K.; Finlay, J. C. Influence of dissolved organic carbon on methylmercury bioavailability across Minnesota stream ecosystems Environ. Sci. Technol. **2011**, 45, 5981– 5987 DOI: 10.1021/es200332f Google Scholar

41. Kolka, R. K.; Grigal, D. F.; Nater, E. A.; Verry, E. S. Hydrologic cycling of mercury and organic carbon in a forested upland-bog watershed Soil Sci. Soc. Am. J. **2001**, 65, 897– 905 DOI: 10.2136/sssaj2001.653897x Google Scholar

42. Mitchell, C. P. J.; Branfireun, B. A.; Kolka, R. K. Total mercury and methylmercury dynamics in upland–peatland watersheds during snowmelt Biogeochemistry **2008**, 90, 225– 241 DOI: 10.1007/s10533-008-9246-z Google Scholar

43. Smith, C. N.; Kesler, S. E.; Blum, J. D.; Rytuba, J. J. Isotope geochemistry of mercury in source rocks, mineral deposits and spring deposits of the California coast ranges, USA Earth Planet. Sci. Lett. **2008**, 269, 398– 406 DOI: 10.1016/j.epsl.2008.02.029 Google Scholar

44. Zheng, W.; Obrist, D.; Weis, D.; Bergquist, B. A. Mercury isotope compositions across North American forests Glob. Biogeochem. Cycles **2016**, 30, 1475– 1492 DOI: 10.1002/2015GB005323 Google Scholar

45. Enrico, M.; Le Roux, G.; Marusczak, N.; Heimbürger, L. E.; Claustres, A.; Fu, X.; Sun, R.; Sonke, J. E. Atmospheric mercury transfer to peat bogs dominated by gaseous elemental mercury dry deposition Environ. Sci. Technol. **2016**, 50, 2405– 2412 DOI: 10.1021/acs.est.5b06058 Google Scholar

46. Jiskra, M.; Wiederhold, J. G.; Bourdon, B.; Kretzschmar, R. Solution speciation controls mercury isotope fractionation of Hg(II) sorption to goethite Environ. Sci. Technol. **2012**, 46, 6654– 6662 DOI: 10.1021/es3008112 Google Scholar

47. Demers, J. D.; Sherman, L. S.; Blum, J. D.; Marsik, F. J.; Dvonch, J. T. Coupling atmospheric mercury isotope ratios and meteorology to identify sources of mercury impacting a coastal urban-industrial region near Pensacola, Florida, USA Glob. Biogeochem. Cycles **2015**, 29, 1689– 1705 DOI: 10.1002/2015GB005146 Google Scholar

48. St. Louis, V. L.; Rudd, J. W. M.; Kelly, C. A.; Hall, B. D.; Rolfhus, K. R.; Scott, K. J.; Lindberg, S. E.; Dong, W. Importance of the forest canopy to fluxes of methyl mercury

and total mercury to boreal ecosystems Environ. Sci. Technol. **2001**, 35, 3089– 3098 DOI: 10.1021/es001924p Google Scholar

49. Timmons, D. R.; Verry, E. S.; Burwell, R. E.; Holt, R. F. Nutrient transport in surface runoff and interflow from an aspen-birch forest J. Environ. Qual. **1977**, 6, 188– 192 DOI: 10.2134/jeq1977.00472425000600020018x Google Scholar

Supporting Information (SI)

New insights on ecosystem mercury cycling revealed by stable isotopes of mercury in water flowing from a headwater peatland catchment

Glenn E. Woerndle [†, Δ], Martin Tsz-Ki Tsui [†], Stephen D. Sebestyen [‡],
Joel D. Blum [‖], Xiangping Nie [§], Randall K. Kolka [‡]

[†] *Department of Biology, University of North Carolina at Greensboro, Greensboro, North Carolina 27402*

[‡] *U.S.D.A. Forest Service, Northern Research Station, Grand Rapids, Minnesota 55744*

[‖] *Department of Earth and Environmental Sciences, University of Michigan, Ann Arbor, Michigan 48109*

[§] *Department of Ecology/Institute of Hydrobiology, Jinan University, Guangzhou 510632, China*

[Δ] Present address (G. E. W.): *School of Earth and Environmental Sciences, Chapman University, Orange, California 92866*

No. of pages: 24
No. of figures: 7
No. of tables: 6

Part I – Description of study site: catchment S2 at MEF

The S2 catchment is a long-term research site in the Marcell Experimental Forest (MEF) managed by the United States Department of Agriculture Forest Service (https://www.nrs.fs.fed.us/ef/marcell). The site and infrastructure are described by Sebestyen et al. [1] and the research program is described by Kolka et al. [2]. The S2 catchment is 9.7 ha, 3.2 ha of which is a peatland dominated by *Sphagnum* species and black spruce (*Picea mariana*), and 6.5 ha of which is forested upland dominated by trembling aspen (*Populus tremuloides*) and paper birch (*Betula alleghaniensis*) (**Fig. S1**).

The bog has Histosol organic soil, with depths ranging from 3 to 7 meters in the interior of the bog.[3] The ombrotrophic bog has a raised-dome surface and the surface of the peatland is perched about 7 m above the surrounding groundwater aquifer in an outwash sand. As such, groundwater does not flow into the peatland, and rainfall and snowfall represent the exclusive water sources to the bog. Streamflow is intermittent and only occurs when the bog water table rises above the elevation of the outlet stream (**Fig. S1**). The stream typically flows from March/April to November/December, and streamflow ceases during periods during most summers. On an annual basis, the bog water table typically fluctuates in the top 30 or less cm of peat, with the surface peat (in microtopographic hollows) being saturated intermittently and sometimes for weeks to months.

Stream stage has been measured by a stripchart recorder at a 120 degree V-notch weir since 1961. Recorded values were verified using weekly point-gage measurements[4] and the weir and gage house datums were re-surveyed every several years.[1] Stage was digitized as sub-daily breakpoint data.[5] We report streamflow as instantaneous values at the time of sampling for regressions (Figures 3 and S4) and show daily streamflow in hydrographs (Figure S4). Streamflow was calculated from a stage-discharge relationship. From the streamflow breakpoint data, we linearly extrapolated between adjacent breakpoint dates/times to estimate instantaneous streamflow at the time of sampling. Streamflow was apportioned into quick and slow flow fractions using a type of recession analysis; the digital recursive hydrograph separation that was described by Nathan and McMahon[6]. Quick/slow flow apportionment is an objective and reproducible analytical approach that can be applied to fixed-interval streamflow time series data. Though it is possible to validate this and similar hydrograph separation approaches as metrics of specific catchment processes,[7] we more generally interpret the apportioned values as a relative measure of runoff from the catchment in response to rainfall or snowmelt. To estimate quick/slow flow amounts, we linearly extrapolated the breakpoint streamflow data to a 30-minute interval time step. We then applied the digital recursive filter at that time step. We selected the nearest half-hourly interval to the sampling time as our

estimate of the quick and slow flow amounts at the time of sampling. To show daily streamflow in a hydrograph, sub-daily streamflow values were aggregated to daily streamflow estimates.

Precipitation and air temperature have been measured since 1961 in a forest clearing within the S2 catchment. Daily precipitation was measured using a NOAH-IV (ETI, Fort Collins, CO) digital recording rain gage. Recording rain gage values were verified and corrected using total weekly precipitation from multiple 8-Inch (20-cm) Standard Rain Gages[8] with Alter wind shields.[9] Air temperature was recorded on paper stripcharts using a Belfort Instrument (Baltimore, MD) Hygrothermograph. Daily minimum and maximum temperatures were read from stripcharts and recorded. Daily mean air temperature was calculated as the mean of the daily minimum and maximum air temperatures. Recorded air temperatures were verified and corrected using weekly readings of paired minimum and maximum thermometers.

Part II – Sample collection at catchment S2

In both 2014 and 2015, we collected water samples every two weeks at the outlet stream, when flowing. We also collected upland runoff from a surface runoff plot and shallow (~30 cm depth) subsurface stormflow from a subsurface runoff plot whenever possible. Though there are both north- and south facing runoff collectors, we only collected upland runoff from a north facing slope in the S2 catchment for this study. Flow from the upland forest at the runoff plots occurs only after events (Fig. S1). Runoff collectors were installed during the 1960s [10] and are described by Sebestyen et al.[1]. Upland runoff includes saturation overland flow, infiltration excess upland runoff (when soils are frozen), and flow through the forest floor and organic horizon. A surface runoff plot (1.8 m x 23.2 m) has galvanized sheet metal to delineate the plot perimeter and water is captured by a galvanized rectangular sheet metal funnel that drains via polyvinyl chloride (PVC) piping to a ~700 L high density polyethylene (HDPE) holding tank. A subsurface runoff plot drains through a stainless steel well screen in a hillslope trench through PVC pipe into a holding tank (**Fig. S1**). Samples were collected from the PVC pipes before the water entered the holding tanks. Two water samples were collected from a PVC piezometer (screened to collect water from 0-10 cm below the hollow surface) in the lagg on the north side of the peatland.

For all water sampling, we triple-rinsed acid-cleaned Teflon bottles (500 mL, 1 L or 2 L) with water, and then filled the bottle(s) without headspace. Bottles were kept on ice and in the dark in a cooler, and shipped overnight to the analytical laboratory at the University of North Carolina at Greensboro (UNCG). In spring 2015, we also collected plant tissue (*see* **Table S4**) and soil core samples to quantify Hg isotope ratios of different potential sources of stream Hg. The samples included litter and one 50-cm core from the bog,

lagg, and the upland forest. We sectioned each core into ten 5-cm increments with a clean stainless steel knife. We also sampled leaf litter or foliage of various tree species in the catchment. All samples were double-bagged and shipped on ice overnight to UNCG.

Concentrations of total organic carbon (TOC) were measured by high-temperature combustion (Standard Method 5310B [11]) on a Shimadzu (Columbia, MD) TOC-V CPH. Potassium hydrogen phthalate (KHP) was used as a reference and check standard. Major cation concentrations and Fe were measured on a Thermo Elemental (West Palm Beach, FL) Iris Intrepid inductively coupled plasma (ICP) optical emission spectrometer (Standard Method 3120 B [11]). Reference and check standards were prepared from Ultra Scientific (North Kingstown, RI) stock solutions for each element. Method detection limits were 0.5 mg C L^{-1} for TOC and 0.01 mg L^{-1} for cations and Fe. Reference standards and analytical duplicates of samples were analyzed after every tenth sample. Cation and TOC concentrations were measured at the USDA Forest Service Forestry Sciences Laboratory in Grand Rapids, MN.

Part III – Total-Hg and MeHg concentration analyses

Unfiltered water samples were completely digested by an acidic mixture of permanganate ($KMnO_4$) and persulfate ($K_2S_2O_8$) in a volumetric proportion of 20 HNO_3:1 H_2SO_4:5 $KMnO_4$ (5% w/v):2.5 $K_2S_2O_8$ (5% w/v) and heated in an oven at 95°C overnight.[12] Digested water samples were cooled, neutralized by 30% hydroxylamine hydrochloride, and weighed aliquots of samples (~40 g) in duplicate were analyzed by the double amalgamation technique and Hg was quantified by cold vapor atomic fluorescence spectrometry (CVAFS; Brooks Rand Model III). A calibration curve (0 to 1 ng) was developed using the NIST-3133 Hg working standard (1 ng Hg mL^{-1}) and was verified by a secondary standard prepared from NIST-1641d (1 ng Hg mL^{-1}). Total-Hg concentrations for the unfiltered water samples were reported in ng Hg per liter (ng L^{-1}), and were also used to calculate the recovery of Hg during purge and trap of water samples for stable Hg isotope analysis.

Unfiltered water samples were preserved with 0.4% (v/v) trace metal grade hydrochloric acid [13] in acid-cleaned 125 mL Teflon bottles and stored at 4°C in the dark until MeHg analysis. Water samples (~50 mL) were distilled to remove matrix interference, buffered with sodium acetate at pH 4.9, and ethylated by 1% sodium tetraethylborate for 25 mins. Alkyl mercury (Hg) species were purged from the bubbler with Hg-free N_2 gas for 12 mins and preconcentrated onto Tenax TA traps. MeHg in water samples was quantified by CVAFS following gas chromatographic separation and pyrolysis.[14,15] The method detection limit (MDL) for MeHg in water samples was established at 0.04 ng L^{-1} for 50 mL of samples analyzed. For water samples

having MeHg below the method detection limit (i.e., 0.04 ng L^{-1}), we assigned a value of half the detection limit (i.e., 0.02 ng L^{-1}) for graphical presentation or calculation.[16] A MeHg calibration standard (1 ng mL^{-1}, supplied by CEBAM Analytical, Inc., Bothell, Washington) was used to develop a calibration curve (0 to 0.5 ng), and the actual MeHg concentration was regularly verified against our in-house total-Hg standard (NIST-3133) using the method outlined by USEPA.[17]

All solid samples were frozen at -20°C immediately upon arriving at UNCG. Frozen samples were then lyophilized in a bench-top freeze-dryer (SP Scientific, Gardiner, NY), and completely homogenized either by an agate mortar and pestle or a mixer mill (SPEX SamplePrep, Metuchen, NJ). All samples were weighed (~0.1 g) and placed in a Teflon digestion vessel (Savillex, Eden Prairie, MN). Vegetation samples were spiked with 5 mL of concentrated trace-metal grade nitric acid (HNO_3) and reagent-grade peroxide (H_2O_2) (4:1; v:v) and lithological samples were spiked with 8 mL of concentrated trace-metal grade hydrochloric acid (HCl) and HNO_3 (3:1; v:v), left overnight in the room with cap loosely tightened, and subsequently amended with 22 mL of 5% BrCl. All samples were then heated at 80°C in a water bath overnight. An aliquot of each digest was neutralized with hydroxylamine and analyzed for total-Hg by CVAFS using the same methods as that for the water samples. For each batch of acid digestions, we included a reagent blank, standard reference materials (SRM NIST-1515 apple leaves, and SRM MESS-3 marine sediment) and duplicates.

Part IV – Validation of our digestion method of high TOC water samples

Previous studies examining stable Hg isotopes in aqueous samples (e.g., precipitation and snow) have used dilute BrCl (e.g., 0.5-5%) to digest aqueous samples at room temperature for an extended period of time in order to completely free Hg from ligands in water samples.[18-22] The BrCl approach is appropriate for precipitation or surface water samples with low organic matter as demonstrated by the relatively high yield of Hg during the extraction process by these studies.

However, in the current study, most water samples had high TOC concentrations (median=79 mg/L; range: 37-116 mg L^{-1}; *n*=23). BrCl may not effectively oxidize all organic matter in the samples before the purge and trap to collect Hg for isotopic analysis, as Hg would be tightly bound to various organic matter pools in these waters.[23] The use of UV oxidization is known to be much more effective in completely breaking down organic matter but may also fractionate Hg isotopes in the samples if Hg is lost from the system.[24] In our study, we sought an alternative method for completely digesting the high-TOC peatland water samples.

We tested an alternative approach that has been previously used to digest samples with high solid loads and organic matter concentrations.[12,25] In that approach, water samples were digested in an acidic mixture of permanganate and persulfate at 95°C overnight.

To verify this digestion approach, we measured total-Hg analyses on two stream water samples from the S2 catchment (collected on September 2, 2014 and on September 16, 2014) using both the BrCl and permanganate/persulfate approaches. The test was completed at the University of Michigan analytical laboratory. We recovered an average of 93% of total-Hg using the digestion method of permanganate / persulfate compared to BrCl /UV oxidation (**Table S1**), assuming the latter approach can destroy all organic matter in the samples. Thus, we consider that our digestion approach provides a high yield of Hg and thus should eliminate or minimize isotopic fractionation of Hg (e.g., MDF) in the peatland water samples during sample processing (e.g., purge and trap).

In addition, digested samples were spiked with a known amount of Hg (50 pg) and re-analyzed for total-Hg concentrations. Post spike analysis recovered between 96-98% from $KMnO_4/K_2S_2O_8$ digested sample *vs.* and 103-104% from the BrCl and UV treatment (**Table S1**). This test provides further evidence that the binding sites in the digested peatland water samples were mostly destroyed (if not all), and that sample Hg should be released upon the addition of stannous chloride ($SnCl_2$) during the purge and trap procedure to separate Hg for isotopic analysis. All Hg analyses for this method comparison were measured using a Nippon MA-2000 cold vapor atomic absorption spectrophotometer (CVAAS) in the analytical laboratory at the University of Michigan.

Part V – Sample processing of environmental samples for stable Hg isotope analyses

After verifying the approach, samples were digested in the analytical laboratory at UNCG. While implementing the purge and trap (**Fig. S2**) at UNCG, we tested the recovery of Hg. We spiked a procedural standard (SRM NIST-3133) into a water sample collected from a local lake with background levels of Hg (Lake Brandt, Greensboro, NC) to verify that our purge and trap system did not inadvertently fractionate Hg isotopes in the sample during processing. Results of three independent tests demonstrated that the purge and trap system resulted in no significant difference in isotopic compositions (δ^{202}Hg: -0.04‰±0.04‰, and Δ^{199}Hg: -0.03‰±0.09‰; *n*=3) from the SRM NIST-3133 isotope solution (δ^{202}Hg: 0.00‰, and Δ^{199}Hg: 0.00‰) we spiked. Therefore, we verified the effectiveness of our purge and trap system for stable Hg isotope analysis.

Digested water samples (permanganate/persulfate approach) were neutralized with 30%

hydroxylamine. About 1 L of neutralized samples were weighed and poured into acid-cleaned 2-L Pyrex borosilicate glass media bottles. In addition, we added 3 mL of 30% hydroxylamine and 100 mL of 50% trace-metal grade sulfuric acid (H_2SO_4). After that, the glass bottles were tightly closed with a 3-hole delivery cap (Pyrex). The first tube (OD: 63.5 mm) served to introduce Hg-free ambient air (through a 0.45-µm syringe filter and a gold trap) into the water, the second tube delivered 10% $SnCl_2$ at ~1 mL min^{-1} controlled by a peristaltic pump, and the third tube directed any Hg(0) in the water to the trap solution (6-7 g by weight or ~5.5 to 6.4 ml) containing 1 % $KMnO_4$ (w/w) in 10 % H_2SO_4 (v/v) (**Fig. S2**). Water samples were continuously stirred on a low-speed stir plate (Corning) and purged by a glass sparger with vacuum created by an Air Cadet pump for about 3 hours. Hg in trap solutions were measured by CVAFS, and recovery of Hg during the purge and trap was calculated and found to be by comparison to the Hg content in the initial samples analyzed after aqueous sample digestions by acids (i.e., concentrated nitric acid and hydrogen peroxide for biological tissues, and aqua regia for soil samples).

Dry and homogenized solid samples were weighed into clean ceramic boats (0.1-1.0 g per boat, max. 2 boats per combustion tube), and packed with layers of Hg-free aluminum oxide (Al_2O_3) and calcium carbonate ($CaCO_3$) powders (Nippon Instruments Corporation). All samples were thermally combusted in a two-stage furnace (the first furnace was ramped from room temperature to 750 ^oC over 6 hours and the second furnace was held at 1,000 ^oC) and released gaseous Hg(0) was collected into 24 g of trap solution containing 1 % $KMnO_4$ (w/w) in 10 % H_2SO_4 (v/v). The initial trap solution was neutralized by hydroxylamine, measured for total-Hg by CVAFS to calculate the recovery of Hg during combustion (typically > 90%). Specifically, our sample combustion recovery averaged at 95.8% with SD of 2.8% (range: 90.8-100.7%), including 18 samples and 6 individual SRM samples (*n*=3 for Mess-3; *n*=3 for NIST-1515) for the current study. Sample Hg would be transferred (upon reduction by 20% $SnCl_2$) into a smaller trap solution (6 to 15 g of 1 % $KMnO_4$ in 10 % H_2SO_4, depending on the total amount of sample Hg) in order to (*i*) separate sample Hg from other combustion products in the initial trap solution, and (*ii*) concentrate Hg in this final solution for Hg stable isotope analysis. Hg in the final trap solution was analyzed for total Hg by CVAFS to determine the recovery of Hg during the transfer step (typically > 90%).

Part VI – Stable mercury isotope analyses

For both water and solid samples, Hg levels in the final trap solution were precisely adjusted to a uniform Hg concentration (± 5 %) along with a bracketing Hg isotope standard (SRM NIST 3133) ranging from 0.5-5 ng g^{-1}.[26] Stable Hg isotope ratios were measured using a Nu Instruments multicollector-

inductively coupled plasma-mass spectrometer (MC-ICP-MS) following methods previously described [26] in the Biogeochemistry and Environmental Isotope Geochemistry Laboratory at the University of Michigan.

Mass-dependent fractionation (MDF) of Hg isotopes is reported as $\delta^{202}Hg$ in permil (‰) referenced to SRM NIST 3133 while mass-independent fractionation (MIF) of Hg isotopes is the difference between the measured $\delta^{202}Hg$ value and the value that would be predicted based on mass dependence. The mass-independent Hg isotope composition is reported as both $\Delta^{199}Hg$ and $\Delta^{201}Hg$ in ‰. Isotopic compositions are calculated according to Blum and Bergquist [26] as:

$$\delta^{202}Hg = \{[(^{202}Hg / {}^{198}Hg)_{sample} \div (^{202}Hg / {}^{198}Hg)_{NIST\ 3133}] - 1\} \times 1000 \quad (S1)$$

$$\Delta^{201}Hg \approx \delta^{201}Hg_{measured} - (\delta^{202}Hg_{measured} \times 0.752) \quad (S2)$$

$$\Delta^{199}Hg \approx \delta^{199}Hg_{measured} - (\delta^{202}Hg_{measured} \times 0.2520) \quad (S3)$$

$$\Delta^{200}Hg \approx \delta^{200}Hg_{measured} - (\delta^{202}Hg_{measured} \times 0.5024) \quad (S4)$$

$$\Delta^{204}Hg \approx \delta^{204}Hg_{measured} - (\delta^{202}Hg_{measured} \times 1.4930) \quad (S5)$$

Analytical uncertainty was determined from replicated analyses of a secondary standard solution (UM-Almadén, mean values: $\delta^{202}Hg$ = -0.56 ‰; $\Delta^{199}Hg$ = -0.03 ‰; *n* = 26), and replicate combustions and analyses of field samples and of SRM NIST-1515 (Apple Leaves) and SRM MESS-3 (Marine Sediment). External analytical reproducibility of $\delta^{202}Hg$ and $\Delta^{199}Hg$ measurements were estimated to be 0.04 to 0.12 ‰ (2 SD) and 0.07 to 0.16 ‰ (2 SD), respectively, based on the repeated analyses of SRM Tort-2 analyzed at different final Hg concentrations on MC-ICP-MS (0.7-5.0 ng g^{-1}).[27]

Table S1 Comparison of total-mercury data for two stream water samples pretreated with BrCl/UV (assumed to result in complete breakdown of organic matter) *vs.* $KMnO_4/K_2S_2O_8$ (our approach) (data reported as mean±S.D.; *n*=3), and the spike recovery of Hg (50 pg) in the treated water samples.

Date of stream sample	Pretreatment	Total-Hg (ng L^{-1})	% Hg released compared to BrCl/UV	Spike Hg recovery (%)
9/2/2014	BrCl/UV	13.8±0.14	100% (assumed)	104
	$KMnO_4/K_2S_2O_8$	12.8±0.12	93%	96
9/16/2014	BrCl/UV	9.5±0.09	100% (assumed)	98
	$KMnO_4/K_2S_2O_8$	8.8±0.26	92%	103

Table S2 Stable mercury isotope compositions (MDF: mass dependent fractionation; MIF: mass independent fractionation) of standard reference materials (SRMs) analyzed for this study, NRCC MESS-3 (Marine Sediment) and NIST-1515 (Apple Leaves).

Site	δ^{202}Hg (‰) [MDF]	Δ^{204}Hg (‰) [MIF]	Δ^{201}Hg (‰) [MIF]	Δ^{200}Hg (‰) [MIF]	Δ^{199}Hg (‰) [MIF]
MESS-3	-1.91	-0.03	-0.09	-0.01	-0.01
	-2.05	0.03	-0.05	0.00	0.01
	-1.90	-0.01	-0.07	-0.03	-0.02
NIST-1515	-2.74	0.06	0.00	-0.01	0.02
	-2.59	-0.03	0.01	0.02	0.07
	-2.69	0.05	-0.02	-0.01	0.04

Table S3 Total-mercury (total-Hg) and stable mercury isotope compositions (MDF: mass dependent fractionation; MIF: mass independent fractionation) of soil cores collected at the catchment S2.

Site	Depth (cm)	total-Hg (ng g^{-1})	δ^{202}Hg (‰) [MDF]	Δ^{204}Hg (‰) [MIF]	Δ^{201}Hg (‰) [MIF]	Δ^{200}Hg (‰) [MIF]	Δ^{199}Hg (‰) [MIF]
Bog (peat) core	0-5	83.9	-2.15	0.04	-0.44	0.06	-0.34
	5-10	133.0	-2.24	0.00	-0.43	0.02	-0.36
	15-20	92.1	-2.06	-0.07	-0.30	0.02	-0.31
	30-35	34.2	-1.46	-0.03	-0.41	-0.05	-0.40
	45-50	39.6	-1.33	-0.02	-0.38	0.02	-0.33
Lagg core	5-10	198.8	-1.88	0.05	-0.35	0.00	-0.39
	20-25	188.3	-1.85	0.07	-0.39	0.03	-0.37
	30-35	171.3	-1.54	-0.08	-0.41	0.08	-0.39
	45-50	108.3	-1.62	-0.01	-0.48	0.04	-0.55
Upland soil core	0-5	91.6	-1.35	-0.11	-0.16	0.03	-0.10
	5-10	31.9	-1.48	-0.06	-0.25	0.00	-0.19
	15-20	16.5	-1.59	0.03	-0.24	0.01	-0.25
	30-35	5.6	-1.55	0.01	-0.41	0.00	-0.37
	45-50	24.6	-1.29	0.09	-0.24	-0.01	-0.30

Table S4 Streamflow, % quick flow, total organic carbon (TOC), total-mercury (total-Hg), methylmercury (MeHg), percent total-mercury as methylmercury (%MeHg), and stable mercury isotope compositions (MDF: mass dependent fractionation; MIF: mass independent fractionation) of stream water samples collected at S2 catchment outlet. ND = not determined.

Date	Streamflow ($L\ s^{-1}$)	% quick flow	TOC ($mg\ L^{-1}$)	Unfiltered total-Hg ($ng\ L^{-1}$)	Unfiltered MeHg ($ng\ L^{-1}$)	%MeHg	$\delta^{202}Hg$ (‰) [MDF]	$\Delta^{204}Hg$ (‰) [MIF]	$\Delta^{201}Hg$ (‰) [MIF]	$\Delta^{200}Hg$ (‰) [MIF]	$\Delta^{199}Hg$ (‰) [MIF]
4/9/2014	0.26	77%	40.5	10.2	<0.04	0.3	-1.48	0.02	-0.22	0.04	-0.19
4/15/2014	2.79	23%	ND	16.7	0.09	0.5	-1.78	-0.13	-0.32	0.01	-0.30
4/23/2014	4.11	22%	40.8	15.5	<0.04	0.2	-1.84	0.19	-0.27	0.14	-0.13
5/13/2014	7.80	52%	51.0	18.6	0.10	0.5	-1.88	0.03	-0.29	0.03	-0.26
5/27/2014	0.13	3%	68.4	13.7	0.27	2.0	-1.72	0.09	-0.28	0.12	-0.22
6/9/2014	0.29	0%	81.2	12.1	0.15	1.2	-1.78	0.02	-0.39	0.05	-0.33
6/23/2014	0.51	0%	81.6	14.8	0.16	1.1	-2.08	0.14	-0.29	-0.04	-0.33
7/7/2014	0.56	43%	93.1	14.9	0.19	1.3	-1.91	-0.03	-0.32	0.09	-0.20
7/21/2014	0.02	0%	84.6	13.4	1.47	11.0	-1.88	0.03	-0.24	0.05	-0.20
9/15/2014	0.003	0%	87.7	8.6	0.38	4.5	-1.76	-0.17	-0.25	0.07	-0.18
9/22/2014	0.02	55%	81.1	12.5	0.38	3.1	-1.82	0.04	-0.36	0.02	-0.25
10/14/2014	0.01	43%	75.3	7.8	0.48	6.1	-1.91	0.04	-0.22	-0.01	-0.27
4/12/2015	0.02	16%	37.0	7.6	0.06	0.9	-1.32	-0.08	-0.24	0.05	-0.12
4/28/2015	0.05	20%	49.1	4.6	0.16	3.5	-1.69	-0.01	-0.26	-0.02	-0.26
5/12/2015	3.99	72%	71.3	9.6	<0.04	0.3	-1.93	-0.01	-0.31	0.01	-0.31
5/26/2015	2.15	65%	65.3	15.5	0.06	0.4	-1.90	-0.06	-0.36	-0.04	-0.29
6/8/2015	3.20	55%	70.7	16.8	0.09	0.6	-1.84	-0.07	-0.34	0.02	-0.26
6/22/2015	0.01	36%	77.2	10.9	0.32	2.9	-1.78	-0.01	-0.15	0.09	-0.18
9/8/2015	5.46	44%	115.5	25.0	0.12	0.5	-1.91	-0.08	-0.38	-0.03	-0.31
9/21/2015	0.03	0%	112.8	10.6	<0.04	0.1	-2.04	0.08	-0.38	0.04	-0.35
10/26/2015	0.17	48%	97.0	10.5	0.08	0.8	-1.80	0.00	-0.35	0.00	-0.22
11/9/2015	0.44	0%	99.3	5.0	0.07	1.3	-2.12	0.31	-0.27	-0.03	-0.30
11/18/2015	4.88	88%	86.2	21.3	0.10	0.5	-1.83	0.00	-0.36	-0.03	-0.33
11/30/2015	0.26	0%	81.6	12.8	0.18	1.4	-1.92	0.03	-0.33	-0.05	-0.31

Table S5 Total-mercury (total-Hg) and stable mercury isotope compositions (MDF: mass dependent fractionation; MIF: mass independent fractionation) of vegetation samples collected at the catchment S2.

Description & location	**total-Hg (ng g^{-1})**	**δ^{202}Hg (‰) [MDF]**	**Δ^{204}Hg (‰) [MIF]**	**Δ^{201}Hg (‰) [MIF]**	**Δ^{200}Hg (‰) [MIF]**	**Δ^{199}Hg (‰) [MIF]**
needles of black spruce (bog)	37.5	-2.27	0.07	-0.56	0.04	-0.48
grass of *Eriophorum spp.* (bog)	18.7	-2.30	0.41	-0.28	0.63	-0.30
needles of tamarack (bog)	36.0	-2.17	0.31	-0.43	0.32	-0.43
leaf litter (upland forest)	32.1	-2.37	0.19	-0.27	0.01	-0.24

Table S6 Total organic carbon (TOC), total-mercury (total-Hg), methylmercury (MeHg), percent total-mercury as methylmercury (%MeHg), and stable mercury isotope compositions (MDF: mass dependent fractionation; MIF: mass independent fractionation) of non-stream water samples collected at the catchment S2

Type of sample	Date	TOC (mg L^{-1})	total-Hg (ng L^{-1})	MeHg (ng L^{-1})	%MeHg	δ^{202}Hg (‰) [MDF]	Δ^{204}Hg (‰) [MIF]	Δ^{201}Hg (‰) [MIF]	Δ^{200}Hg (‰) [MIF]	Δ^{199}Hg (‰) [MIF]
Upland runoff	4/12/2015	52.7	56.8	0.06	0.1	-1.37	-0.01	-0.28	0.05	-0.19
Upland runoff	5/12/2015	ND	18.3	<0.04	0.1	-1.18	0.12	-0.33	0.05	-0.22
Subsurface stormflow	4/23/2014	14.8	16.9	ND	ND	-1.41	-0.29	-0.20	-0.07	-0.29
Subsurface stormflow	6/3/2015	19.6	23.0	0.07	0.3	-1.48	-0.03	-0.34	0.03	-0.24
Subsurface stormflow	11/18/2015	33.5	23.9	0.09	0.4	-1.34	-0.01	-0.25	0.05	-0.24
Lagg porewater	4/12/2015	37.5	13.1	0.27	2.1	-1.32	0.03	-0.34	-0.01	-0.25
Lagg porewater	5/12/2015	53.4	10.4	0.33	3.2	-1.71	-0.04	-0.32	-0.01	-0.25

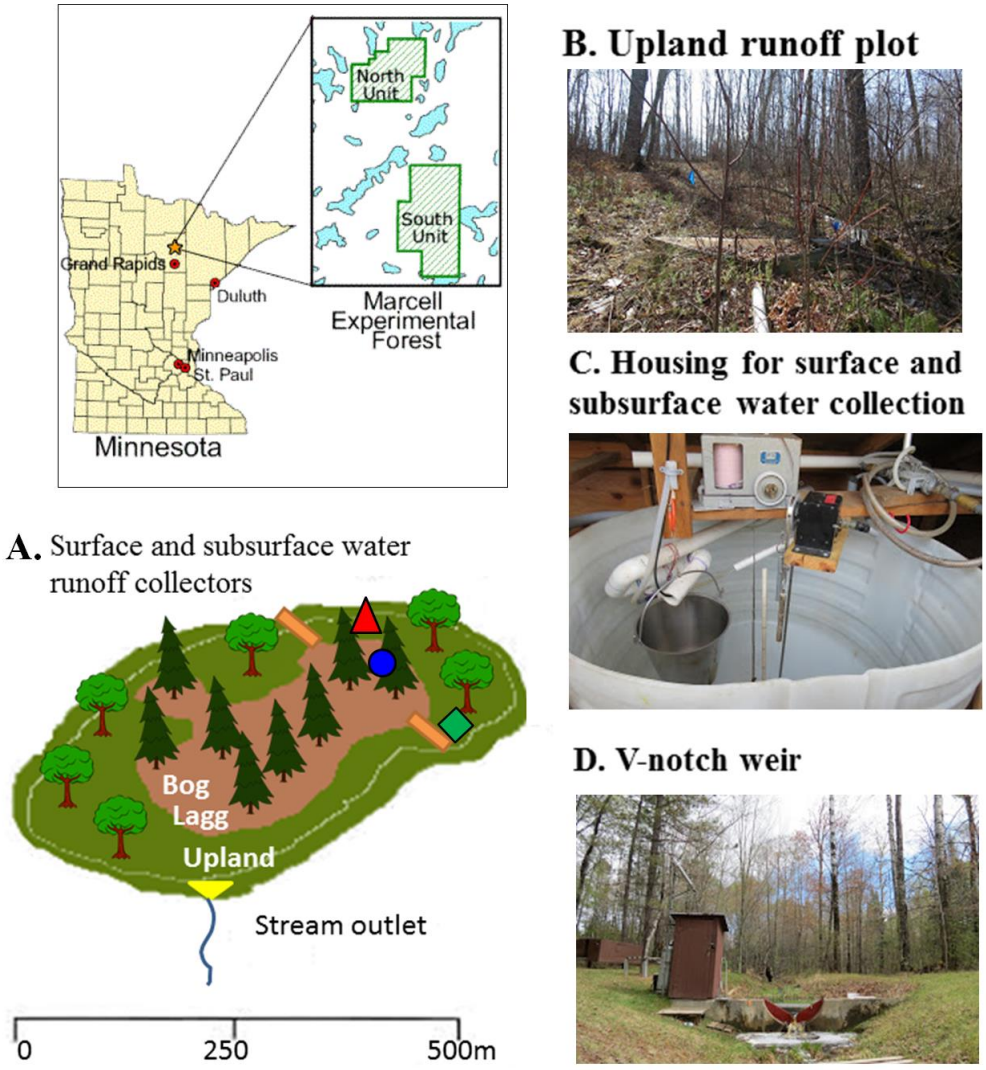

Fig. S1 (A) The S2 catchment includes an upland forest, bog, and lagg area and a V-notch weir at the watershed outlet. Boardwalk is shown in yellow/orange strip. Sampling locations of the three cores and associated vegetation samples (next to each core sampled) are shown as bog core in blue circle, lagg core in red triangle, and upland core in green diamond. **(B)** Upland runoff and shallow subsurface stormflow were collected from runoff plots on the north-facing upland hillslope. **(C)** Both surface and subsurface runoff is stored in a shelter with tanks and recording instruments that measure the amount of runoff at the time of sample collection. **(D)** Watershed S2 export waters were collected from a V-notch weir at the catchment outlet when the stream was flowing. The water table level was continuously monitored and recorded on a strip chart in the housing unit near the V-notch weir. Daily precipitation and air temperature were also recorded.

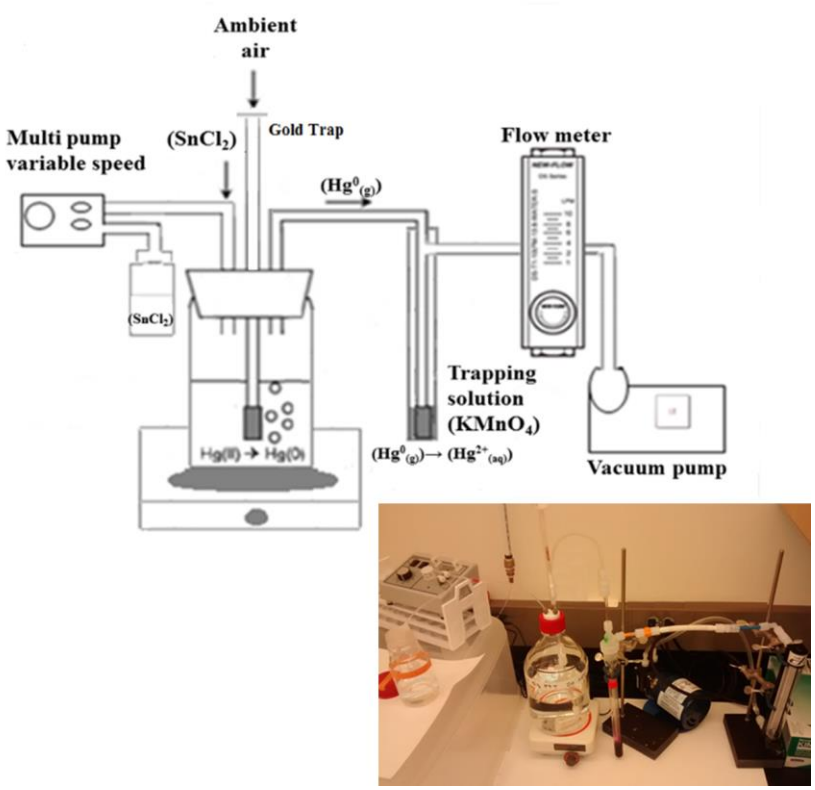

Fig. S2. Purge and trap method following sample digestion. Approximately 1 L of digested water was placed in a 2 L acid-cleaned borosilicate media bottle with a Corning three-hole delivery cap. The10% $SnCl_2$ reductant was continuously and slowly added to the stirred solution to reduce Hg^{2+}(aq) into Hg^0(g). A vacuum directed the reduced Hg^0 (g) into a 1% $KMnO_4$ trap solution that oxidized Hg^0(g) to Hg^{2+}(aq), and trapped Hg was later analyzed using CVAFS to determine "purge and trap" recovery as well as analyzed using MC-ICP-MS for determining Hg stable isotope ratios in the sample.

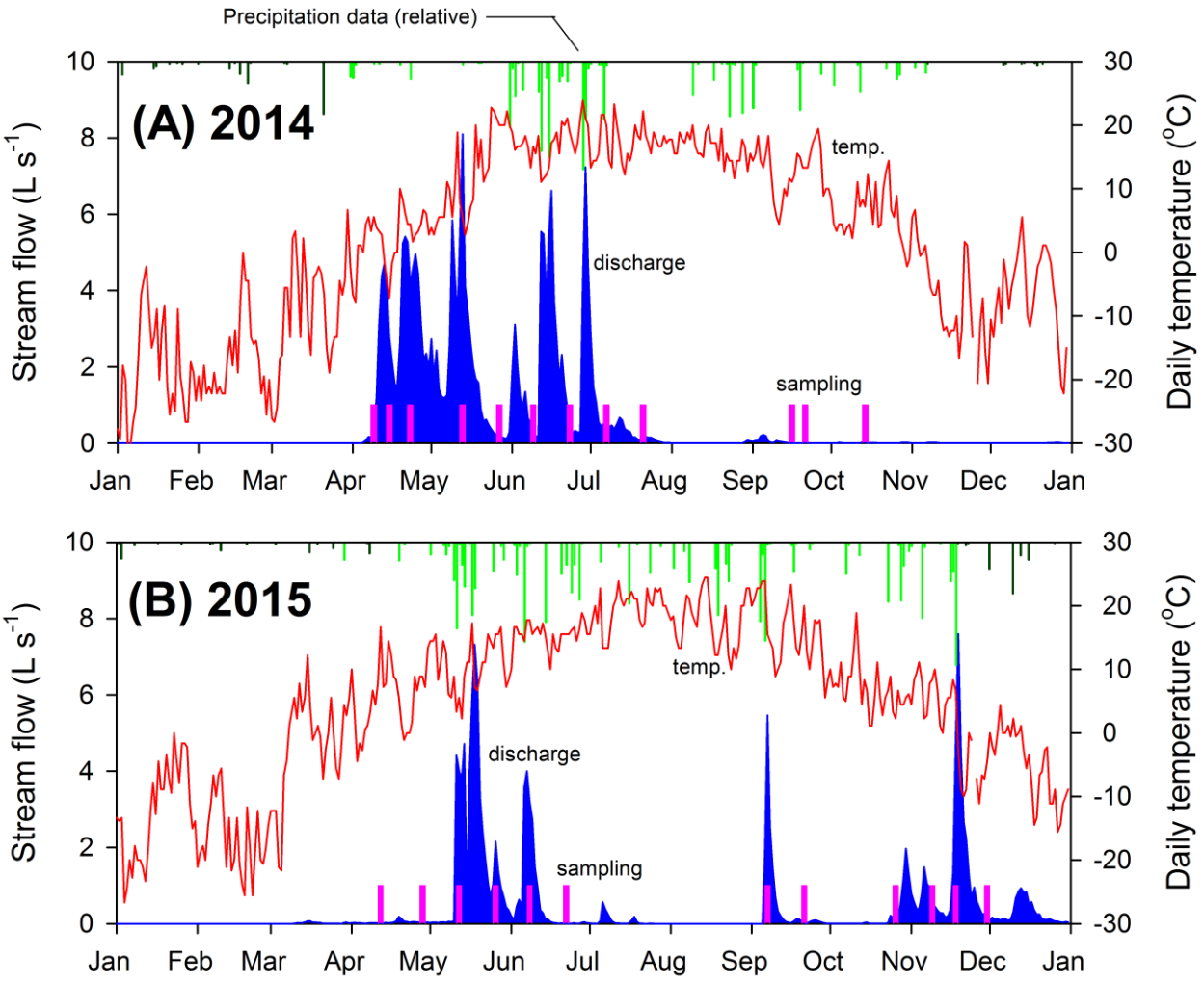

Fig. S3 Streamflow (in blue) at the outlet of the S2 catchment and the daily mean air temperature (in red) (**A**) 2014 and (**B**) 2015, as well as the relative precipitation (in green, from the top of the figure), grey shows snow fall and green shows rainfall amount, pink bars shows when stream water samples were collected at the outlet of S2 catchment (*n*=12 per year).

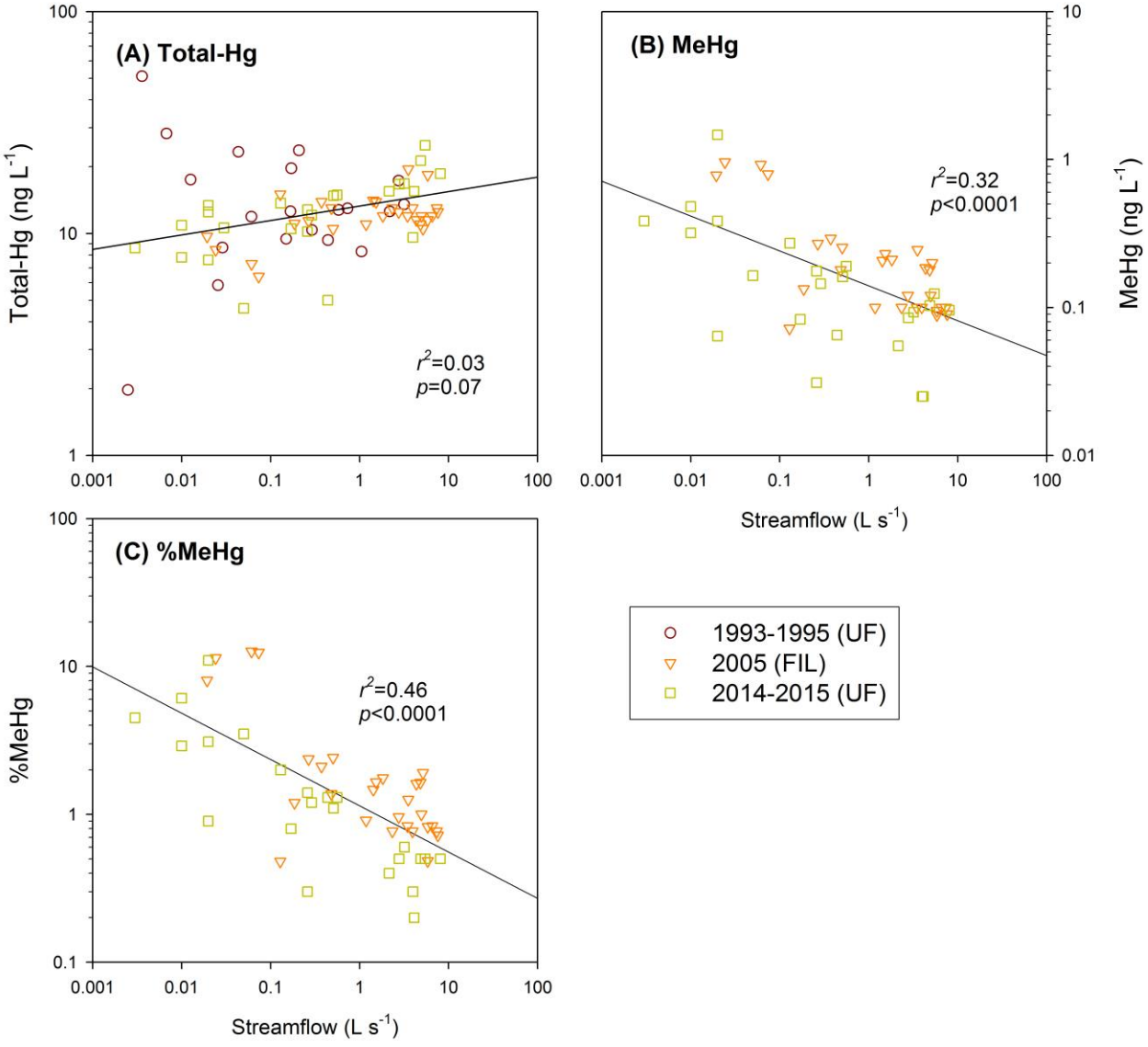

Fig. S4 The relationship of log_{10}-transformed streamflow with **(A)** log_{10}-transformed total-mercury concentrations, **(B)** log_{10}-transformed methylmercury concentrations, and **(C)** log_{10}-transformed %MeHg (percent total-mercury as methylmercury) in stream water collected in this study and other published studies at the catchment S2.[28,29] Note: UF = unfiltered; FIL = filtered (0.45-µm).

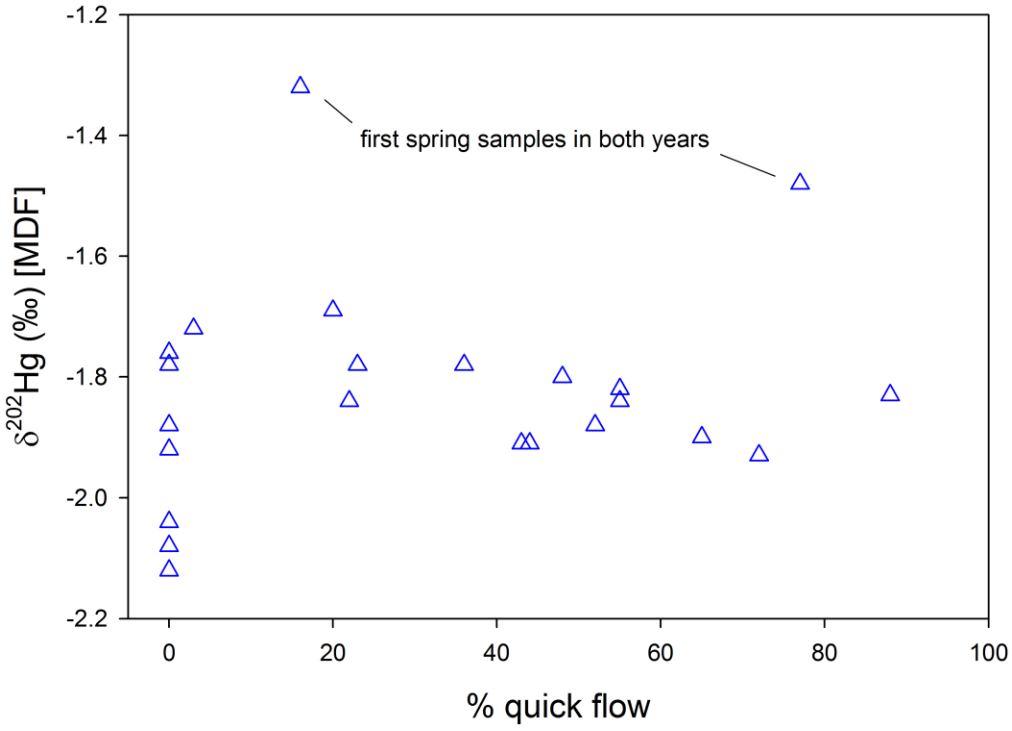

Fig. S5 Relationship between mass-dependent fractionation (MDF) of stable mercury isotopes and % quick flow in stream waters.

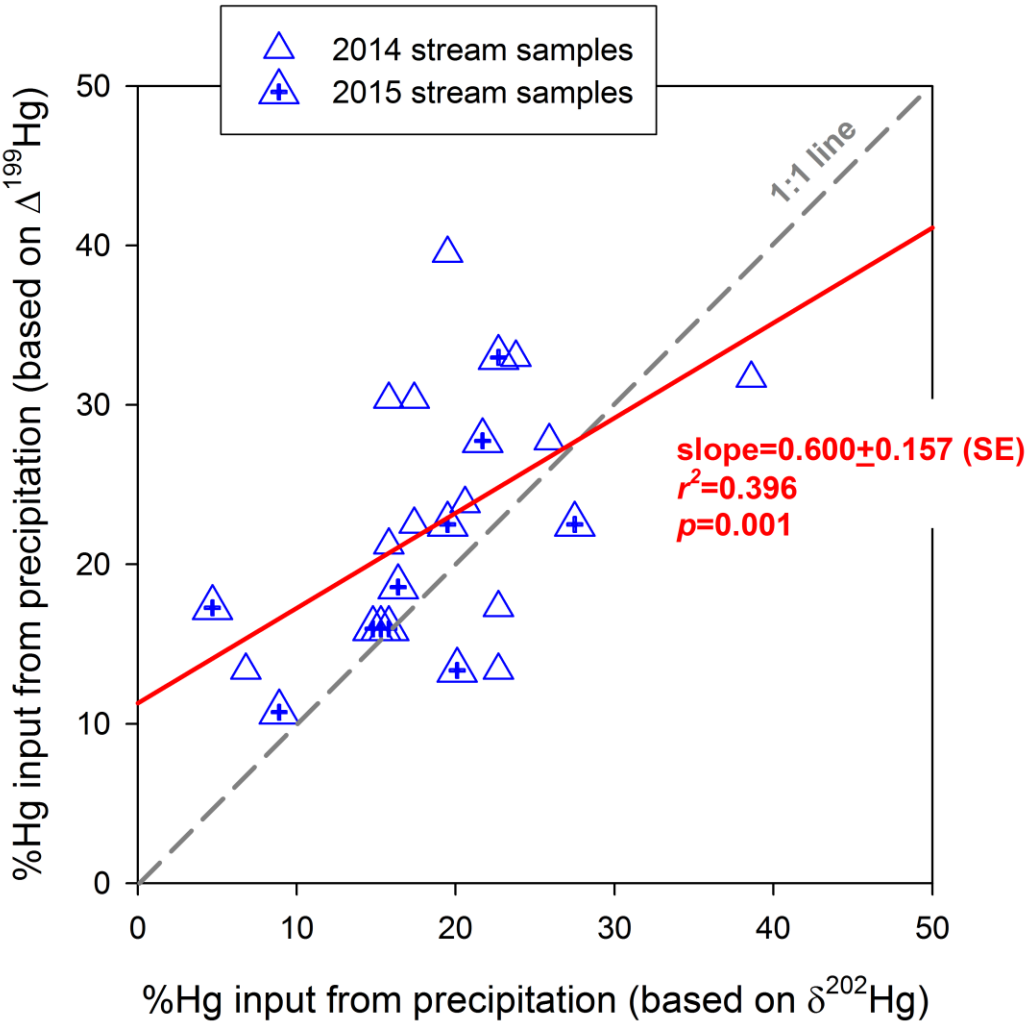

Fig. S6 Comparison of the estimated %Hg input from precipitation to stream water at the catchment S2 in this study from binary mixing model based on mass-dependent fractionation (MDF; as δ^{202}Hg) values *vs.* odd-mass mass-independent fractionation (MIF; as Δ^{199}Hg) values in stream water samples.

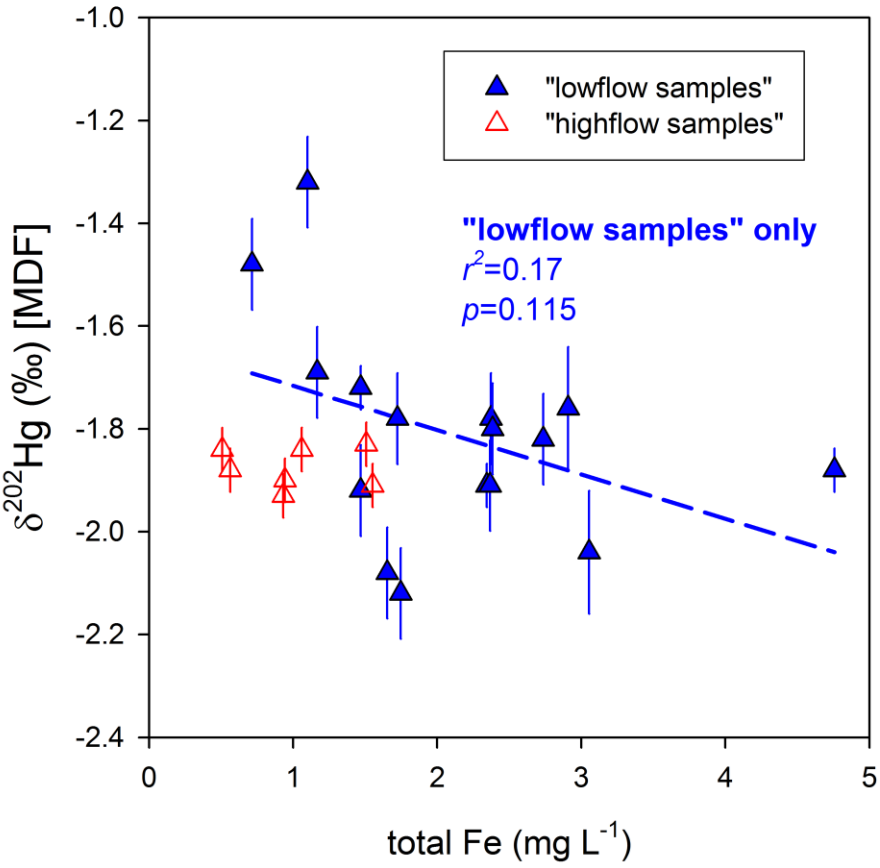

Fig. S7 Relationship between mass-dependent fractionation (MDF) of stable mercury isotopes and total iron in stream waters during different flow regimes as defined in Fig. 3 in main text.

References (Supporting Information)

1. Sebestyen, S. D.; Dorrance, C.; Olson, D. M.; Verry, E. S.; Kolka, R. K.; Elling, A. E.; Kyllander, R. Long-term monitoring sites and trends at the Marcell Experimental Forest. In: Kolka, R. K.; Sebestyen, S. D.; Verry, E. S.; Brooks, K. N. (eds.) *Peatland Biogeochemistry and Watershed Hydrology at the Marcell Experimental Forest*. 2011. CRC Press, Boca Raton, FL.
2. Kolka, R. K.; Sebestyen, S. D.; Bradford, J. H. (2011) An evolving research agenda of the Marcell Experimental Forest. In: Kolka, R. K.; Sebestyen, S. D.; Verry, E. S.; Brooks, K. N. (eds.) *Peatland Biogeochemistry and Watershed Hydrology at the Marcell Experimental Forest*. 2011. CRC Press, Boca Raton, FL.
3. Verry, E. S.; Janssens, J. Geology, vegetation, and hydrology of the S2 bog at the MEF: 12,000 years in northern Minnesota. In: Kolka, R. K.; Sebestyen, S. D.; Verry, E. S.; Brooks, K. N. (eds.) Peatland Biogeochemistry and Watershed Hydrology at the Marcell Experimental Forest. 2011. CRC Press, Boca Raton, FL.
4. Brakensiek, D. L.; Osborn, H. B.; Rawls, W. J. Field manual for research in agricultural hydrology, Agriculture handbook, 550 pp. 1979. US Department of Agriculture, Washington, D.C.
5. Johnson, E. A.; Dils, R. E. Outline for compiling precipitation, runoff, and ground water data from small watersheds, Station Paper, 40 pp. 1956. Southeastern Forest Experiment Station, Asheville, NC.
6. Nathan, R. J.; McMahon, T. A. Evaluation of automated techniques for base flow and recession analyses. *Water Resour. Res.* **1990**, *26*, 1465-1473.
7. Shanley, J. B.; Sebestyen, S. D.; McDonnell, J. J.; McGlynn, B. L.; Dunne, T. Water's Way at Sleepers River watershed - revisiting flow generation in a post-glacial landscape, Vermont USA. *Hydrol. Process.* **2015**, *29*, 3447-3459.
8. US Weather Bureau. Measurement of precipitation: instructions on the measurement and registration of precipitation by means of the standard instruments of the U. S. Weather Bureau. Circular E. US Weather Bureau. **1913**. Washington, DC, p 37.
9. Alter, J. C. Shielded storage precipitation. *Mon. Weather Rev.* **1937**, *66*, 262-265.
10. Timmons, D. R.; Verry, E. S.; Burwell, R. E.; Holt, R. F. Nutrient transport in surface runoff and interflow from an aspen-birch forest. *J. Environ. Qual.* **1977**, *6*, 188-192.
11. APHA. Standards Methods for the Examination of Water and Wastewater. American Public Health Association / American Waters Works Association / Water Environment Federation, Washington, DC. 1995.
12. Balogh, S. J.; Meyer, M. L.; Johnson, D. K. Mercury and suspended sediment loadings in the lower Minnesota River. *Environ. Sci. Technol.* **1997**, *31*, 198-202.
13. Parker, J. L.; Bloom, N. S. Preservation and storage techniques for low-level aqueous mercury speciation. *Sci. Total Environ.* **2005**, *337*, 253-263.
14. Bloom, N. Determination of picogram levels of methylmercury by aqueous phase ethylation, followed by cryogenic gas chromatography with cold vapour atomic fluorescence detection. *Can. J. Fish. Aquat. Sci.* **1989**, *46*, 1131-1140.

15. Horvat, M.; Liang, L.; Bloom, N. S.; Comparison of distillation with other current isolation methods for the determination of methyl mercury compounds in low level environmental samples. Part II. Water. *Anal. Chim. Acta.* **1993**, *282*, 153-168.

16. Clarke, J. U. Evaluation of censored data methods to allow statistical comparisons among very small samples with below detection limit observations *Environ. Sci. Technol.* **1998**, *32*, 177-183.

17. USEPA. Method 1631, Revision E: Mercury in Water by Oxidation, Purge and Trap, and Cold Vapor Atomic Fluorescence Spectrometry. Office of Water. EPA-821-R-02-019. **2002.** Washington, D.C.

18. Gratz, L. E.; Keeler, G. J.; Blum, J. D.; Sherman, L. S. Isotopic composition and fractionation of mercury in Great Lakes precipitation and ambient air. *Environ. Sci. Technol.* **2010**, *44*, 7764-7770.

19. Sherman, L. S.; Blum, J. D.; Johnson, K. P.; Keeler, G. J.; Barres, J. A.; Douglas, T. A. Mass-independent fractionation of mercury isotopes in Arctic snow driven by sunlight. *Nat. Geosci.* **2010**, *3*, 173-177.

20. Chen, J., Hintelmann, H., Feng, X., Dimock, B. (2012) Unusual fractionation of both odd and even mercury isotopes in precipitation from Peterborough, ON, Canada. *Geochimica et Cosochimica Acta* 90: 33-46

21. Sherman, L. S.; Blum, J. D.; Keeler, G. J.; Demers, J. D.; Dvonch, J. T. Investigation of local mercury deposition from a coal-fired power plant using mercury isotopes. *Environ. Sci. Technol.* **2012**, *46*, 382-390.

22. Demers, J. D.; Blum, J. D.; Zak, D. R. Mercury isotopes in a forested ecosystem: Implications for air-surface exchange dynamics and the global mercury cycle. *Glob. Biogeochem. Cycles* **2013**, *27*, 222-238.

23. Ravichandran, M. Interactions between mercury and dissolved organic matter – A review. *Chemosphere* **2004**, *55*, 319-331.

24. Mead, C.; Lyons, J. R.; Johnson, T. M.; Anbar, A. D. Unique Hg stable isotope signatures of compact fluorescent lamp-sourced Hg. *Environ. Sci. Technol.*, **2013**, *47*, 2542-2547.

25. Balogh, S. J.; Nollet, Y. H. Mercury mass balance at a wastewater treatment plant employing sludge incineration with offgas mercury control. *Sci. Total Environ.* **2008**, *389*, 125-131.

26. Blum, J. D.; Bergquist, B. A. Reporting of variations in the natural isotopic composition of mercury. *Anal. Bioanal. Chem.* **2007,** *388*, 353-359.

27. Tsui, M. T. K.; Blum, J. D.; Kwon, S. Y.; Finlay, J. C.; Balogh, S. J.; Nollet, Y. H. Photodegradation of methylmercury in stream ecosystems. *Limnol. Oceanogr*. **2013**, *58*, 13-22.

28. Kolka, R. K.; Grigal, D. F.; Nater, E. A.; Verry, E. S. Hydrologic cycling of mercury and organic carbon in a forested upland–bog watershed. *Soil Sci. Soc. Am. J.* **2001**, *65*, 897-905.

29. Mitchell, C. P. J.; Branfireun, B. A.; Kolka, R. K. Total mercury and methylmercury dynamics in upland–peatland watersheds during snowmelt. *Biogeochemistry* **2008**, *90*, 225-241.